JOURNAL OF VIROLOGY, Mar. 2005, p. 3146–3162 Vol. 79, No. 5
0022-538X/05/$08.00+0 doi:10.1128/JVI.79.5.3146–3162.2005

Transfer of the Full-Length Dystrophin-Coding Sequence into Muscle Cells by a Dual High-Capacity Hybrid Viral Vector with Site-Specific Integration Ability

Manuel A. F. V. Gonçalves,[1]* Gijsbert P. van Nierop,[1] Marloes R. Tijssen,[1] Pierre Lefesvre,[2] Shoshan Knaän-Shanzer,[1] Ietje van der Velde,[1] Dirk W. van Bekkum,[2] Dinko Valerio,[1] and Antoine A. F. de Vries[1]

Gene Therapy Section, Department of Molecular Cell Biology, Leiden University Medical Center,[1] and Crucell N.V.,[2] Leiden, The Netherlands

Received 3 June 2004/Accepted 8 October 2004

Duchenne muscular dystrophy (DMD) is caused by mutations in the *DMD* gene, making it a potential target for gene therapy. There is, however, a scarcity of vectors that can accommodate the 14-kb *DMD* cDNA and permanently genetically correct muscle tissue in vivo or proliferating myogenic progenitors in vitro for use in autologous transplantation. Here, a dual high-capacity adenovirus–adeno-associated virus (hcAd/AAV) vector with two full-length human dystrophin-coding sequences flanked by AAV integration-enhancing elements is presented. These vectors are generated from input linear monomeric DNA molecules consisting of the Ad origin of replication and packaging signal followed by the recently identified AAV DNA integration efficiency element (p5IEE), the transgene(s) of interest, and the AAV inverted terminal repeat (ITR). After infection of producer cells with a helper Ad vector, the Ad DNA replication machinery, in concert with the AAV ITR-dependent dimerization, leads to the assembly of vector genomes with a tail-to-tail configuration that are efficiently amplified and packaged into Ad capsids. These dual hcAd/AAV hybrid vectors were used to express the dystrophin-coding sequence in rat cardiomyocytes in vitro and to restore dystrophin synthesis in the muscle tissues of *mdx* mice in vivo. Introduction into human cells of chimeric genomes, which contain a structure reminiscent of AAV proviral DNA, resulted in AAV Rep-dependent targeted DNA integration into the *AAVS1* locus on chromosome 19. Dual hcAd/AAV hybrid vectors may thus be particularly useful to develop safe treatment modalities for diseases such as DMD that rely on efficient transfer and stable expression of large genes.

The lethal X-linked recessive disorder Duchenne muscular dystrophy (DMD) is the most frequent inherited muscle disease affecting ca. 1 in 3,500 newborn males. DMD is a consequence of mutations in the *DMD* gene encoding the 427-kDa dystrophin protein. In normal myofibers, dystrophin anchors the internal cytoskeleton to a protein complex in the plasma membrane that is in turn connected with components of the extracellular matrix (4). The absence of this structural link in dystrophin-defective muscle fibers contributes to disruption of the sarcolemma upon mechanical stress. Damaged muscle fibers are transiently repaired through expansion and fusion of resident satellite cells. After exhaustion of the satellite cell pool, the muscle tissue is replaced by adipose and connective tissues. Relentless progression of the disease causes affected individuals to be wheelchair-bound at around 12 years of age and to die generally in their early twenties because of cardiac or respiratory muscle failure.

Although somatic gene therapy can potentially eradicate the cause of recessive monogenetic disorders by delivering functional copies of the defective genes into afflicted cells, the genetic complementation of DMD presents unique challenges due to the large size of the *DMD* mRNA (14 kb), as well as the large volume of the muscle system. Tackling the latter hurdle involves testing improved strategies to systemically deliver in vivo either gene transfer vectors or cells with myogenic potential. Simultaneously, recombinant genes encoding microdystrophins are being constructed that aim at retaining maximum functionality and fit within small viral gene delivery vehicles such as adeno-associated virus (AAV) and retrovirus vectors (45). Recent studies in transgenic mice suggest that microdystrophins might be effective in blocking ongoing muscle injury, although they may not achieve complete muscle strength restoration (21). Moreover, the extent to which microdystrophins rescue the dystrophic phenotype in larger animals and humans is unknown. AAV vectors in particular are, nonetheless, promising therapeutic gene carriers because they can transduce nondividing cells, lack viral genes encoding immunogenic proteins, and achieve long-term transgene expression in immunocompetent animal models of human diseases such as muscular dystrophies (18, 21). In addition, they are based on a defective nonpathogenic human virus that can site specifically integrate its DNA into a defined region of the human genome (30, 43) designated *AAVS1* (29). Integration into this chromosome 19 locus depends on the interaction of the AAV Rep78 or Rep68 proteins with specific Rep-binding sites in the AAV inverted terminal repeats (ITRs) (7, 33), in the recently identified integration efficiency element (p5IEE) (38, 39) that overlaps with

* Corresponding author. Mailing address: Gene Therapy Section, Department of Molecular Cell Biology, Leiden University Medical Center, Wassenaarseweg 72, 2333 AL Leiden, The Netherlands. Phone: 31-71-5271971. Fax: 31-71-5276180. E-mail: m.goncalves@lumc.nl.

the AAV promoter at map position 5 (p5) (33), and in the *AAVS1* locus (54). This feature of AAV biology is unique among all known eukaryotic viruses and its exploitation holds considerable promise for the targeted integration and stable expression of therapeutic DNA. However, incorporation of the AAV site-specific DNA integration machinery into conventional AAV vectors would further reduce their already limited coding capacity thus requiring the use of even smaller microdystrophins for DMD gene therapy, which are unlikely to be effective. An alternative route to DMD gene therapy is the development of improved high-capacity adenovirus (hcAd) vectors that not only permit delivery of the full-length *DMD* cDNA and thus synthesis of completely functional dystrophin but also include genetic elements to increase their performance. Since hcAd vectors retain from the parental virus only the signals involved in DNA replication and encapsidation, their amplification and assembly relies on packaging-defective helper Ad vectors to provide in *trans* nonstructural and structural proteins, respectively. Importantly, hcAd vectors preserve the unsurpassed gene transfer efficiency into dividing and nondividing cells of their earlier generation counterparts but lack viral genes that makes them more spacious, safer, and better suited for prolonged transgene expression (28). These attributes have been spurring a steady improvement of the hcAd vector system (36, 44, 51). Recently, a dual hcAd vector was generated by packaging in Ad capsids a molecularly cloned tandem of two *DMD* cDNA expression units containing the CAG promoter. At present, this construction achieves the highest expression of the full-length *DMD* open reading frame (ORF) in skeletal muscle of *mdx* mice (11, 12). However, since DNA delivered by Ad vectors usually remains episomal, they are not suited for long-term genetic correction of dystrophin-defective myogenic progenitor (34) or candidate muscle stem cell populations (25, 42, 46). The therapeutic application of these progenitors as an expandable source of transplantable autologous myogenic cells will require their permanent genetic modification. This can best be accomplished through transgene integration into host chromosomal DNA. Preferably, the integrated DNA should not harbor genetic elements with outward enhancer/promoter activity, as present in retroviral long terminal repeats, to avoid oncogene activation. Ideally, the integration event should target a predefined site within the human genome to reduce the risk of insertional mutagenesis.

We describe here a new hc virus vector system that expands the utility of hcAd vectors by endowing them with the ability to site specifically integrate foreign DNA and by doubling the number of transgene copies packaged in each particle. Using these so-called dual hcAd/AAV hybrid vectors, efficient delivery and expression of the full-length human dystrophin-coding sequence in synchronously beating rat primary cardiomyocytes was accomplished. We further showed restoration of full-length dystrophin protein synthesis in gastrocnemius muscles of the *mdx* DMD mouse model in vivo. Finally, in proof-of-concept experiments with human cervical carcinoma cells, we have demonstrated that dual hcAd/AAV hybrid vectors can be used, together with the AAV Rep78 and Rep68 proteins, to target foreign genetic information into the *AAVS1* locus.

MATERIALS AND METHODS

Recombinant DNA. Recombinant DNA techniques were performed by using established methods (41) or according to the instructions supplied with specific reagents. All hc vector DNA templates were inserted in a pBR322-derived cloning vector. First, plasmid pBR-HD-RE1.d5 was made. This shuttle construct contains nucleotides 1 through 454 of the human Ad serotype 5 (Ad5) genome. This 454-bp region encompasses the left ITR plus packaging signal and was PCR amplified by using the primer set and DNA template presented elsewhere (15). These Ad *cis*-acting sequences are followed by the AAV serotype 2 (AAV2) region from nucleotide positions 153 through 300, which encompass the p5IEE and p5 promoter. This 147-bp sequence was obtained through PCR amplification by using pBR.RepCap.TAA-Not as a template and PR127 (5′-CCATCGATTGGAGTCG TGACGTGAATTACGTCATAGGGTTAGGGAGGTCCTGTATT AGAGGTC ACG-3′) and PR128 (5′-CCACTAGTCCCGCTTCAAAATGGAGACC-3′) as primers. Plasmid pBR.RepCap.TAA-Not contains residues 191 through 4492 of the wild-type AAV2 genome but has the ATG codon at position 321 replaced by the stop codon TAA. Downstream of the p5 sequence lies the Ad5 region from nucleotide position 35533 through 35938. This 405-bp 3′-terminal noncoding sequence includes the right Ad5 ITR region and was PCR amplified by using template pWE/AflII-rITR.pac.Rfib5 (26), together with the primers PR25 (5′-GCCACTGC AGCCTTACCAGTAAAAAAGAAAAC-3′) and PR26 (5′-ACCTGGGCCCATC ATCAATAATATACCTTA). The PCR amplifications of the Ad and AAV *cis*-acting elements were performed with Platinum *Taq* DNA Polymerase High Fidelity (Invitrogen), and the absence of mutations in the PCR-amplified sequences was confirmed by DNA sequencing. Next, plasmid pBR/NC-RE1.d5 was derived from pBR/HD-RE1.d5 by substituting the 405-bp 3′-terminal Ad5 sequence with a DNA fragment containing the 145-bp AAV2 ITR. The latter DNA was derived from pAAV/AdTRΨ.5 (15). Subsequently, a fragment consisting of the human elongation factor 1α (*EF1*α) gene promoter from pEFO (a gift of L.-M. Houdebine [48]), a polylinker and the rabbit β-*globin* gene pA from pCAGGS (kindly provided by J.-i. Miyazaki [35]) was cloned between the p5IEE and the 3′ Ad ITR in pBR/HD-RE1.d5 and between the p5IEE and the AAV ITR in pBR/NC-RE1.d5. These maneuvers gave rise to constructs pBR/HD-RE1.EF and pBR/NC-RE1.EF, respectively. Next, the *EGFP-dystrophin* ORF was purified from pDysE (a gift from J. Tremblay [6]) and inserted into the polylinker of both pBR/HD-RE1.EF and pBR/NC-RE1.EF, yielding pAd.eDYS and pAd/AAV.eDYS, respectively. The shuttle plasmids pAd.DsRed and pAd/AAV.DsRed were derived from pAd.eDYS and pAd/AAV.eDYS, respectively, by substituting the enhanced green fluorescent protein (EGFP)-coding portion of the *EGFP-dystrophin* DNA with a fragment containing a red fluorescent protein (*DsRed*) ORF and the simian virus 40 (SV40) pA. The latter fragment was obtained from pDsRed.T4-N1 (made available by B. Glick [3]). Finally, plasmids pAd.EGFP and pAd/AAV.EGFP were derived from pAd.eDYS and pAd/AAV.eDYS, respectively, by substituting the EGFP coding portion of the *EGFP-dystrophin* DNA with a fragment containing the *EGFP* ORF and the human growth hormone gene pA. The *EGFP* ORF came from plasmid pEGFP (Clontech), whereas the human growth hormone pA was obtained from construct pEFO. The construct pKS.P5.Rep contains the AAV2 *rep* under the control of its endogenous promoters and hence codes for the Rep78, Rep68, Rep52, and Rep40 proteins. Plasmid pGAPDH.Rep78/68 directs the synthesis of Rep78 and Rep68 only, because of the introduction at AAV2 genome position 993 of the triplet GGG in place of the Rep52 and Rep40 initiation codon. The human glyceraldehyde 3-phosphate dehydrogenase gene promoter was obtained from plasmid pGAP489CAT (a gift from S. Yanagisawa [1]). Complete nucleotide sequences of all constructs are available upon request.

Cells. Growth conditions for the human cervical carcinoma (HeLa) cells (American Type Culture Collection) and the Ad5 early region 1 (E1)- and bacteriophage P1 *cre*-expressing PER.tTA.Cre76 cells have been previously described (16). Cultures of spontaneously contracting neonatal rat cardiomyocytes were kindly provided by A. van der Laarse. Procedures for the establishment and maintenance of these cultures are described elsewhere (52). All cells were kept in a humidified air–10% CO_2 atmosphere at 37°C.

First-generation Ad vectors. The generation, purification, and titration of the Ad vectors Ad.floxedΨ and Ad.ΔE1.EGFP with E1 deleted have been detailed elsewhere (16, 17).

Packaging assay for hc vector DNA encoding the red fluorescent protein. Four million PER.tTA.Cre76 cells in Dulbecco modified Eagle medium (DMEM; Invitrogen) supplemented with 10% fetal bovine serum (FBS; Invitrogen) and 10 mM $MgCl_2$ were seeded in wells of six-well plates (Greiner). Subsequently, semiconfluent monolayers were transfected in triplicate with 2.5 μg of pAd/AAV.DsRed alone or with 2.5 μg of pAd/AAV.DsRed and 0.5 μg of the AAV *rep* expression plasmid pKS.P5.Rep. Positive control samples consisted of PER.tTA.Cre76 cells transfected with 2.5 μg of the conventional hcAd vector shuttle

plasmid pAd.DsRed alone or together with 0.5 μg of pKS.P5.Rep. Prior to transfection, pAd/AAV.DsRed and pAd.DsRed were digested with MssI (Fermentas), followed by restriction enzyme heat inactivation for 15 min at 65°C. Before addition to the cells, the plasmids were diluted in DMEM to a final volume of 100 μl. Next, the DNA solutions were mixed with 100 μl of a cationic liposome suspension consisting of 10 μl of Lipofectamine (Invitrogen) and 90 μl of DMEM. The DNA-liposome complexes were allowed to form at room temperature for 30 min. In the mean time, the monolayers were rinsed with 1 ml of DMEM. Subsequently, the DNA-liposome complexes were diluted in DMEM to a final volume of 1 ml and added to the washed cells. After a 3-h incubation period at 37°C, 1 ml of DMEM supplemented with 20% FBS and 20 mM $MgCl_2$ was added to the culture wells. After overnight incubation, the transfection medium was replaced by fresh DMEM containing 10% FBS, 10 mM $MgCl_2$, and Ad.floxedΨ at a multiplicity of infection (MOI) of 3 infectious units (IU)/cell. After incubation for 5 h at 37°C, the inoculum was removed, and 3.5 ml of DMEM supplemented with 10% FBS plus 10 mM $MgCl_2$ was added to the cells. Upon detection of complete cytopathic effect (CPE), ca. 72 h postinfection (p.i.), the cells were harvested and subject to three cycles of freezing (liquid nitrogen bath) and thawing (37°C water bath). Next, the cellular debris was pelleted by centrifugation at 208 × *g* for 10 min, and the resulting supernatants were clarified by filtration through 0.45-μm-pore-size Millex-HA filters (Millipore). *DsRed* gene transfer efficiencies were determined by flow cytometric analyses as follows. HeLa cells were seeded at a density of 10^5 cells per well in 24-well plates (Greiner). After overnight incubation, the confluent cell layers received 500 μl of fivefold serially diluted clarified lysates. Two days later, the cells were analyzed for *DsRed* expression by using a FACSort flow cytometer (Becton Dickinson). In all instances, 10,000 events were acquired and stored in list mode files and analyzed by using CellQuest software (Becton Dickinson Immunocytometry Systems). Gene transfer activities were calculated from the linear range of the dose-response curves. Mock-infected HeLa cells were used to determine background signal intensities.

Assembly, propagation, and quantification of dual hcAd/AAV hybrid vectors encoding the EGFP-dystrophin fusion protein. Dual hcAd/AAV.eDYS particles were amplified by serial propagation on PER.tTA.Cre76 cells. The initial rescue and assembly (rescue/assembly) steps (designated P0) were performed with MssI-linearized pAd/AAV.eDYS by the same method as for the DsRed-encoding hc vectors. Next, one-tenth of the primary dual hcAd/AAV.eDYS stock was mixed with fresh culture medium and added to 5.0×10^6 newly seeded PER.tTA.Cre76 cells in wells of six-well plates together with Ad.floxedΨ at an MOI of 2 IU/cell. After incubation for 5 to 6 h, the inoculum was replaced by 3.5 ml of DMEM supplemented with 10% FBS and 10 mM $MgCl_2$. The producer cells were harvested after detection of CPE (normally 3 to 4 days p.i.). The aforementioned procedure was repeated during subsequent passages with 7.0×10^6 PER.tTA.Cre76 cells in 25-cm^2 flasks (Greiner) for passage P2, 2.2×10^7 PER.tTA.Cre76 cells in 75-cm^2 flasks (Greiner) for passage P3, and 8.7×10^7 PER.tTA.Cre76 cells in 175-cm^2 flasks (Greiner) for passage P4. For each round of propagation, one-tenth of clarified lysate from the previous passage was used.

Purified stocks of hybrid vector particles were prepared from clarified lysates of ca. 2.6×10^8 PER.tTA.Cre76 cells in 12 75-cm^2 flasks at the third round of propagation (P3). The purification scheme consisted of CsCl buoyant-density ultracentrifugation followed by three ultrafiltration cycles using Amicon-Ultra centrifugal filters (Millipore) to exchange the CsCl solution for phosphate-buffered saline (PBS) containing 7% glycerol. Prior to ultracentrifugation, the clarified producer cell lysates were incubated with DNase I (Roche) at 25 μg/ml for 30 min at 37°C. Vector stocks were divided in 50-μl aliquots that were snap-frozen in liquid nitrogen and stored at −80°C.

The concentrations of functional dual hcAd/AAV.eDYS particles in purified hybrid vector stocks were determined by endpoint titrations on HeLa cells using flow cytometry and on Ad.floxedΨ-infected PER.tTA.Cre76 cells by using flow cytometry and direct fluorescence microscopy. A total of 10^5 HeLa cells were seeded in wells of 24-well plates. After overnight incubation, the confluent cell layers received 500 μl of fivefold serial dilutions of dual hcAd/AAV.eDYS hybrid vector stocks. Two days later, the cells were analyzed for *EGFP-dystrophin* expression with a FACSort flow cytometer as described above. A total of 5×10^5 PER.tTA.Cre76 cells were seeded in duplicate in wells of 24-well plates. After overnight incubation, the confluent cell layers received Ad.floxedΨ at an MOI of 2 IU/cell, together with fivefold serial dilutions of hybrid vector stocks. After a 4-h incubation at 37°C, the plates were subjected to centrifugation for 20 min at 1,500 × *g*, after which the inocula were replaced with fresh culture medium. The cells in one plate were incubated for 20 h prior to flow cytometry analyses. PER.tTA.Cre76 cells infected with AdfloxedΨ only, were used to determine the background signal intensities. The cell layers in the other plate were covered with a 3.0-ml agarose overlay prepared by mixing 9.0 ml of phenol red-free 2× minimal essential medium (Invitrogen), 0.36 ml of FBS, 0.18 ml of 1 M $MgCl_2$, 1.3 ml of PBS, and 7.2 ml of 2.5% (wt/vol) SeaPlaque agarose (FMC). Gene transfer activities in the latter plate were determined at 20 and 120 h p.i. by counting EGFP-dystrophin-positive cells and foci, respectively, with the aid of an Olympus IX51 inverse fluorescence microscope.

Extrachromosomal DNA extraction. The purification of extrachromosomal DNA was performed as previously described (15).

Extraction of dual hcAd/AAV hybrid vector DNA. Aliquots of a purified hybrid vector stock were treated with DNase I at a final concentration of 0.3 μg/μl for 30 min at 37°C in the presence of 10 mM $MgCl_2$. Subsequently, the nuclease was inactivated by addition of EDTA (pH 8.0), sodium dodecyl sulfate, and proteinase K (Roche) to final concentrations of 10 mM, 0.5%, and 0.1 μg/μl, respectively. The samples were then incubated at 56°C for 1 h and extracted twice with a mixture of Tris-buffered phenol, chloroform, and isoamyl alcohol (25:24:1) and once with chloroform. The hybrid vector DNA was recovered by ethanol precipitation.

Southern blot analysis. After agarose gel electrophoresis, DNA was transferred by capillary action to a nylon membrane (Hybond-XL; Amersham Biosciences). All DNA probes were labeled with [α-^{32}P]dCTP (Amersham Biosciences) by using the HexaLabel DNA labeling system (Fermentas).

Transduction of neonatal rat cardiomyocytes and immunofluorescence microscopy. Approximately 2×10^5 neonatal rat heart cells seeded on glass coverslips in wells of six-well plates were transduced either with dual hcAd/AAV.eDYS or with Ad.ΔE1.EGFP vectors at MOIs of 10^3 focus-forming units (FFU)/cell and 10^2 IU/cell, respectively. Ad.ΔE1.EGFP is a first-generation Ad5-based vector containing in place of E1 the *EGFP* ORF under the transcriptional control of the human cytomegalovirus immediate-early promoter and the SV40 pA (17). Negative control samples consisted of mock-transduced cells. Dual hcAd/AAV.eDYS hybrid vector particles were also used to transduce HeLa cells at an MOI of 2×10^2 FFU/cell. After overnight incubation, the cardiomyocyte cultures were washed twice with PBS and replenished with fresh medium. At 2 days p.i. the transduced and mock-transduced cultures were washed twice with PBS for 5 min. The cells were fixed with 4% (vol/vol) paraformaldehyde in PBS for 15 min at room temperature. The fixative was removed by four 5-min washes with 10 mM glycine in PBS (PBSG). Next, the cells were permeabilized by a 5-min treatment with 1% (vol/vol) Triton X-100 in PBS at room temperature. The detergent was removed by three 5-min washes with PBSG. Subsequently, a blocking step was performed by incubating the cells for 1 h with PBSG containing 5% FBS. A monoclonal antibody (MAb) directed against the cardiac-specific marker cardiac troponin-I (cTNI; HyTest) was diluted 1:100 in PBSG with 5% FBS. After overnight incubation at 4°C, the cells were rinsed three times with PBS and stained with a Cy3-conjugated donkey anti-mouse immunoglobulin G (IgG) (H+L) antibody (Jackson Immunoresearch Laboratories) diluted 1:100 in PBSG containing 5% FBS. After a 45-min incubation at 4°C, excess secondary antibody was removed by four washes with PBS. Cell nuclei were stained with Hoechst 33342 (Molecular Probes) at a final concentration of 10 μg/ml in PBS. The cells were incubated for 5 min in the dark at 4°C and, subsequently, the Hoechst 33342 solution was removed by four washes with PBS. The specimens were laid on a drop of Vectashield (Vector Laboratories) on a glass slide and examined by using an Olympus IX51 inverse fluorescence microscope. Digital images were acquired by using a ColorView II Peltier-cooled charge-coupled device color camera and analySIS software (Soft Imaging System). Images were merged in Adobe Photoshop version 5.0.

Skeletal muscle immunohistochemistry. Dual hcAd/AAV.eDYS hybrid vector particles (2×10^8 FFU) in 100 μl of PBS containing 7% glycerol were injected with a 30-gauge needle into the left gastrocnemius muscle of 6-week-old C57BL/10ScSn-*Dmd*^{mdx}/J mice. Gastrocnemius muscles of C57BL/10ScSn and C57BL/10ScSn-*Dmd*^{mdx}/J mice were injected with 100 μl of PBS with 7% glycerol and used as positive and negative controls for the immunohistochemical staining procedure, respectively. Experimentation with animals was executed in compliance with a study protocol approved by the animal ethics committee of the Leiden University Medical Center. Whole gastrocnemius muscles were collected at 6 days postinjection and snap-frozen in liquid nitrogen. Serial transverse cryostat sections with a thickness of 10 μm and spanning the entire length of the muscle were obtained every 30 μm. The sections were allowed to dry overnight at 37°C. After rehydration, the sections were immersed in methanol containing 0.035% H_2O_2 for 20 min and subsequently rinsed with PBS. The sections were incubated for 45 min in PBS supplemented with 4% bovine serum albumin (BSA) to prevent nonspecific staining. Human dystrophin was detected by immunohistochemistry using the mouse MAb NCL-DYS2 (Novocastra) directed against the C terminus of the protein. This MAb of the IgG1 isotype (a gift of I. Ginjaar) was diluted 1:40 in PBS containing 1% BSA and labeled with 20-fold-diluted horseradish peroxidase (HRPO)-conjugated Fab fragments by using a

Zenon HRPO mouse IgG1 labeling kit (Molecular Probes). Next, the antibody mixture was added to the specimens without further dilution, followed by incubation for 60 min at room temperature. After a washing step, the sections were fixed with 4% formaldehyde in PBS for 30 min and again rinsed with PBS. The antibody complexes were visualized by incubation of the sections in 20 mM sodium acetate (pH 5.2) containing 5% dimethylformamide, 400 μg of 3-amino-9-ethylcarbazole (Sigma)/ml, and 0.02% H_2O_2. Rinsing the specimens with water stopped the enzymatic reaction. Subsequently, the sections were counterstained with hematoxylin-eosin and mounted in Aquamount (BDH) for light microscopic evaluation. Negative controls consisted of tissue sections that underwent the entire staining procedure but were incubated with HRPO-conjugated Fab fragments diluted 40-fold in PBS containing 1% BSA instead of HRPO-labeled NCL-DYS2.

Site-specific DNA integration assay. A total of 8×10^4 HeLa cells were seeded in wells of 24-well plates. After overnight incubation, the cells were transfected with 0.5 μg of either pKS.P5.Rep, pGAPDH.Rep78/68, or pEFO.DsRed.T4 by using 2.4 μl of ExGen500 (Fermentas) according to the instructions of the manufacturer. Cells transfected with the latter construct served both as a *rep*-negative control and as a control for the DNA transfection procedure. Transfected HeLa cells were transduced with dual hcAd/AAV.eDYS hybrid vector particles at three different MOIs (i.e., 18, 90, and 450 FFU/cell). After a 2-h incubation the cells were washed with PBS and, at 3 days p.i., were harvested and genomic DNA was extracted as described previously (17). Samples containing 240 ng of chromosomal DNA were subjected to PCR with the *AAVS1*-specific primer pAAVS1b (24), together with primer Beta.R1 (5′-GCCAGATTTTTCC TCCTCTCC-3′) targeting the rabbit β-*globin* gene pA present in the dual hcAd/AAV chimeric genome. Each primer was used at a final concentration of 0.2 μM. PCR mixtures containing 2% (vol/vol) deionized formamide, 200 μM deoxynucleoside triphosphates, and 2.5 U SuperTaq DNA polymerase (HT Biotechnology) were placed in an UNO-thermoblock (Biometra), and a touchdown PCR program was initiated by a 3-min incubation at 94°C, followed by 20 cycles of 94°C for 60 s, an annealing period of 60 s with the temperature decreasing by 0.5°C every cycle from 69 to 59°C, and a 2-min extension step at 72°C. When the PCR program reached the lower annealing temperature of 59°C, 28 additional cycles were carried out by using the above-mentioned cycling conditions except for the use of a constant annealing temperature of 59°C. The reactions were finished by a 10-min incubation at 72°C. Subsequently, 3 μl of each PCR sample was subjected to a seminested PCR with the *AAVS1*-specific primer Cr2-AAVS1 (5′-ACAATGGCCAGGGCCAGGCAG-3′), together with oligodeoxyribonucleotide Beta.R1. The same cycling conditions as described above were applied for the seminested PCR, after which, two 3-μl fractions of each reaction mixture were subjected to agarose gel electrophoresis. Next, each set of resolved DNA fragments was transferred through capillary action to Hybond-XL membranes. One membrane was incubated with a 677-bp hybrid vector DNA-specific probe, whereas the other membrane was exposed to a 353-bp *AAVS1*-specific probe. The 677-bp probe includes the Ad ITR, the Ad packaging signal, and the p5IEE and hybridizes with the 5′ terminus of the hybrid vector DNA. The 353-bp probe was obtained by PCR amplification of genomic DNA extracted from PER.C6 cells (10) with the primers pr.s1.s2 (5′-CAGGTCCACCCTCTGCTG-3′) and pr.s1.as (5′-GGCTCAACATCGGAAGAG-3′) using the aforementioned cycling conditions. Both probes were purified by using the QIAEX II gel extraction kit (Qiagen). In parallel, the PCR products were purified from gel and inserted into pCR4-TOPO (Invitrogen) by using the TOPO TA cloning system (Invitrogen). The resulting recombinant plasmids were digested with EcoRI. Subsequently, the digestion products corresponding to the pCR4-TOPO plasmid backbone and to the amplified *AAVS1*-hybrid vector DNA junctions were resolved in duplicate by agarose gel electrophoresis. Afterwards, Southern blot analyses with either the 677-bp hybrid vector DNA-specific probe or the 353-bp *AAVS1*-specific probe were performed. Finally, the nucleotide sequences of several cloned PCR fragments were determined as previously described (16) by using primers T3 (5′-ATTAACCCTCACTAAAGGGA-3′) and T7 (5′-TAATA CGACTCACTATAGGG-3′).

RESULTS

Packaging of dual hcAd/AAV hybrid vector DNA. The complex involved in AAV DNA replication acts on AAV ITRs flanking either wild-type AAV sequences or recombinant DNA to generate unit-length, as well as double-length linear duplex molecules termed monomeric and dimeric AAV replicative forms, respectively. The dimeric structures arise when AAV Rep78- or Rep68-dependent nicking at the terminal resolution site (trs) of the AAV ITR fails prior to the reinitiation of DNA synthesis (23). We reasoned that we could exploit this AAV ITR hairpin-dependent dimerization process and couple it to the Ad DNA replication machinery to assemble in producer cells Ad replicons with a tail-to-tail structure encoding two copies of a transgene flanked by the AAV DNA integration-promoting elements p5IEE and ITR. Our hypothesis was that the 5′ Ad ITR would provide an origin of replication for the Ad DNA polymerase complex, whereas the 3′ AAV ITR hairpin structure would cause this complex to turn around and generate covalently bound double-stranded tail-to-tail dimers. In addition, by judicious size selection of the input Ad/AAV hybrid vector DNA, the dimerization process would assure the generation of molecules greater than the ~28-kb lower genome size limit required for efficient Ad DNA packaging (37) but smaller than the maximum size that fits in Ad capsids (2).

To this end, the shuttle plasmid pAd/AAV.DsRed was constructed (Fig. 1A). In this plasmid, the human *DMD* ORF and a *DsRed* gene expression unit are framed by the Ad ITR and packaging signal plus the aforementioned AAV elements (Fig. 1A). Plasmid pAd.DsRed, which codes for a regular hcAd vector DNA, contains from the Ad genome exclusively both termini, including the origins of replication (located within the ITRs) and the packaging elements (Fig. 1A). This construct was used as a positive control template in the rescue/assembly experiments described below. Prior to transfection, pAd/AAV.DsRed and pAd.DsRed were digested to completion with MssI. MssI digestion releases the Ad ITRs from most of the plasmid backbone turning them into much more efficient substrates for the initiation of Ad DNA-dependent replication than undigested templates (22). MssI-digested pAd.DsRed and pAd/AAV.DsRed were transfected into the E1-complementing PER.tTA.Cre76 cells (16) alone or together with an AAV *rep* expression plasmid (pKS.P5.Rep). The Rep78 and Rep68 proteins bind to the AAV ITRs and assist in the initiation of replication of both wild-type and recombinant AAV genomes by excising them from flanking covalently linked nonviral DNA. Monitoring of DsRed-positive PER.tTA.Cre76 cells by fluorescence microscopy revealed comparable transfection efficiencies in each of the experiments (not shown). Next, Ad helper activities necessary for the amplification and packaging of recombinant DNA templates were provided in *trans* by infection with Ad.floxedΨ. Ad.floxedΨ is an E1-deleted Ad vector whose packaging signal is bracketed by a direct repeat of bacteriophage P1 *loxP* sites. In PER.tTA.Cre76 cells that constitutively express the P1 Cre recombinase, assembly of Ad.floxedΨ particles is prevented to a great extent by Cre/*loxP*-mediated excision of the Ad packaging elements (16). After the emergence of CPE, producer cell cultures were harvested and cleared lysates were used to infect HeLa indicator cells. At 2 days p.i. reporter gene transfer efficiencies were determined through fluorescence-activated flow cytometry. The lysates corresponding to cells transfected with pAd/AAV.DsRed and pKS.P5.Rep showed the highest reporter gene transfer activity (Fig. 1B). Samples derived from cells that received pAd.DsRed and pKS.P5.Rep had 15.5% ± 6.2% of the gene transfer activity present in specimens from pAd/AAV.DsRed- and pKS.P5.Rep-transfected cells. The lysates of cell cultures transfected either with pAd.DsRed or pAd/AAV.DsRed alone

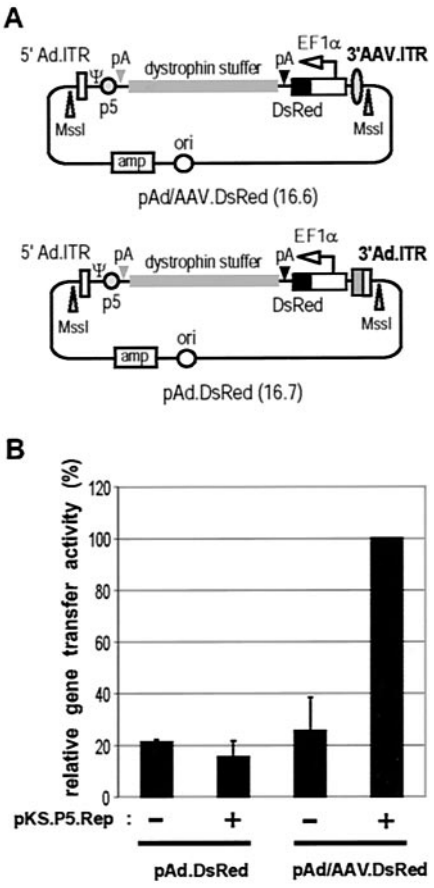

FIG. 1. (A) Schematic representation of the hc vector shuttle constructs pAd.DsRed and pAd/AAV.DsRed. The structure of pAd/AAV.DsRed differs from that of pAd.DsRed by the presence of an AAV ITR in place of the 3′ Ad ITR. Arrowhead, MssI recognition site; open box, Ad ITR (Ad5 nucleotide positions 1 through 103); Ψ, Ad packaging signal-containing sequence (Ad5 genome positions 104 through 454); shaded circle, p5IEE sequence (AAV2 nucleotide positions 153 through 300); shaded triangle, β-*globin* gene pA; shaded bar, stuffer DNA consisting of the human dystrophin-coding sequence; solid triangle, SV40 pA; solid box, *DsRed* ORF; open box with arrow, *EF1*α gene promoter; shaded oval, AAV ITR (AAV2 genome positions 1 through 145); shaded box, Ad5 nucleotide positions 35533 through 35835; amp, β-*lactamase* gene; ori, prokaryotic origin of replication. The numbers in parentheses correspond to the sizes (in kilobases) of the hc vector DNA released from the plasmid backbones after digestion with MssI. (B) Flow cytometric analyses on HeLa indicator cells of the relative reporter gene transfer activities in cell lysates derived from Ad.floxed.Ψ-infected PER.tTA.Cre76 cells initially transfected either with MssI-treated pAd.DsRed or pAd/AAV.DsRed alone or with MssI-digested pAd.DsRed or pAd/AAV.DsRed together with pKS.P5.Rep ($n = 3$). The variation in the number of DsRed-positive cells between samples derived from PER.tTA.Cre76 cultures transfected with MssI-digested pAd/AAV.DsRed and pKS.P5.Rep (fourth bar of the graph) was no more than 36%.

displayed reporter gene transfer efficiencies of 21.2% ± 1.1% and 25.5% ± 13.2%, respectively, of that achieved with samples derived from pAd/AAV.DsRed- and pKS.P5.Rep-transfected cells. Negative control samples corresponding to transfected cells that were not infected with Ad.floxedΨ did not lead to reporter gene expression above background (not shown). From these experiments, we conclude that it is possible to incorporate into Ad capsids Ad/AAV chimeric genomes and that AAV Rep proteins, although not required, do enhance the rescue/assembly process.

Structure of dual hcAd/AAV hybrid vector replicative forms. In the next set of experiments, we investigated the structural organization of replicative hybrid vector DNA. To this end, we constructed pAd/AAV.eDYS. This plasmid has exactly the same arrangement of Ad and AAV *cis*-acting elements as pAd/AAV.DsRed. However, instead of controlling *DsRed* transcription, the *EF1*α gene promoter drives expression of a recombinant gene encoding a fusion product of the EGFP and the full-length human dystrophin proteins (Fig. 2A). Construct pAd/AAV.eDYS was derived from pAd.eDYS (Fig. 2A), encoding a conventional hcAd vector genome, by substituting the 3′ Ad-specific segment with an AAV ITR. Consequently, the EGFP-dystrophin-encoding hcAd and hcAd/AAV genomes differ from each other only at their 3′ termini. The packaging of EGFP-dystrophin-encoding hc vector DNA was initiated by transfecting MssI-digested pAd/AAV.eDYS or MssI-digested pAd.eDYS into PER.tTA.Cre76 cells. The producer cells were subsequently infected with Ad.floxedΨ. After the development of CPE, the cell cultures were harvested and newly seeded PER.tTA.Cre76 producer cells were inoculated with one-tenth of each cleared lysate. The Ad helper functions were again provided in *trans* by Ad.floxedΨ. The negative control consisted of newly seeded PER.tTA.Cre76 cells infected with Ad.floxedΨ alone. After an incubation period of 48 h, extrachromosomal DNA was extracted from the cells, digested with BamHI or EcoRV and subjected to Southern blot analyses with two vector-specific DNA probes (Fig. 2A). Shuttle plasmid pAd/AAV.eDYS digested with the same restriction enzymes provided positive control templates for DNA probe hybridizations. Digestion with BamHI generated fragments of 0.7, 8.6, and 10.6 kb (Fig. 2B, lane 1), whereas EcoRV treatment yielded products of 1.9, 2.4, 6.9, and 8.6 kb (Fig. 2B, lane 2) after incubation with a mixture of both probes. All of these fragments are predicted from the restriction map of non-MssI-digested, circular, pAd/AAV.eDYS. Both BamHI- and EcoRV-treated extrachromosomal DNA from PER.tTA.Cre76 cells infected with Ad.floxedΨ alone did not produce any hybridization signal confirming the specificity of both probes (not shown). Using the same combination of probes, extrachromosomal DNA from two independent rescue/assembly and propagation experiments started with MssI-treated pAd.eDYS yielded products of 0.7, 2.7, 4.5, and 8.6 kb when digested with BamHI (Fig. 2B, lanes 3 and 5) and of 1.9, 2.4, 4.8, and 6.9 kb after digestion with EcoRV (Fig. 2B, lanes 4 and 6). These results show a preponderance of unit-length vector DNA replicative forms after one round of propagation of hcAd.eDYS particles in permissive cells. Under the same conditions, Southern blot analyses of extrachromosomal DNA from three independent rescue/assembly and propagation experiments with MssI-digested pAd/AAV.eDYS using probe 2832 alone or together with probe 6563 revealed the presence of an additional EcoRV fragment of 9.0 kb (Fig. 2B, lanes 8, 10, 12, and 16). These particular DNA species corresponds to replicative DNA forms with a tandem tail-to-tail organization (Fig. 2C). Treatment of extrachromosomal DNA with BamHI produced 8.6-kb internal dystrophin-coding segments that did not resolve sufficiently from the expected 8.4-kb dimer-specific DNA fragments (Fig. 2B, lanes 7, 9, and 11). We confirmed the presence of

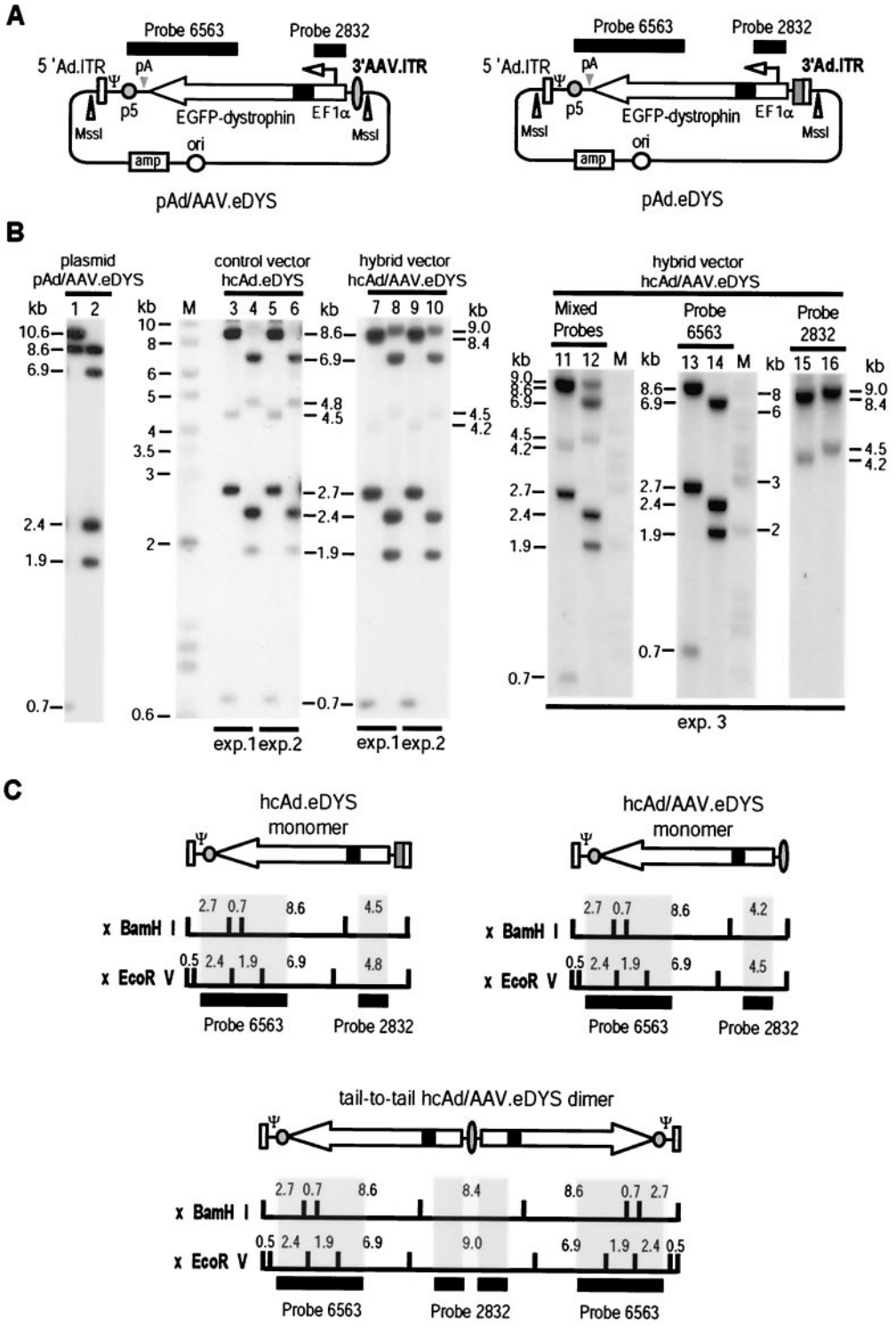

FIG. 2. (A) Schematic representation of the hc vector shuttle constructs pAd.eDYS and pAd/AAV.eDYS. The structure of pAd/AAV.eDYS differs from that of pAd.eDYS by the presence of an AAV ITR in place of the 3′ Ad ITR. Large open arrow, human dystrophin-coding sequence in frame with the *EGFP* ORF (solid box); solid bars, DNA probes 6563 and 2832 drawn in relation to their target DNA sequences. For an explanation of the other symbols and abbreviations, see the legend for Fig. 1A. (B) Structural analysis of replicative DNA forms generated during the first round of propagation on Ad.floxedΨ-infected PER.tTA.Cre76 cells of control (lanes 3 to 6) and hybrid (lanes 7 to 16) hc vector particles derived from MssI-digested pAd.eDYS and MssI-treated pAd/AAV.eDYS, respectively. The extrachromosomal DNA molecules from three independent rescue/assembly and propagation experiments (exp.1, exp.2, and exp.3) were digested either with BamHI (lanes 3, 5, 7, 9, 11, 13, and 15) or with EcoRV (lanes 4, 6, 8, 10, 12, 14, and 16). Control samples consisted of the shuttle plasmid pAd/AAV.eDYS digested either with BamHI (lane 1) or with EcoRV (lane 2). Lanes M, GeneRuler DNA Ladder Mix molecular weight marker (Fermentas). After agarose gel electrophoresis, the resolved DNA fragments were subjected to Southern blotting and DNA hybridizations by using probe 6563 (lanes 13 and 14), probe 2832 (lanes 15 and 16), or a mixture of these probes (lanes 1 through 12). (C) BamHI and EcoRV restriction maps of the monomeric hcAd.eDYS, monomeric hcAd/AAV.eDYS and tail-to-tail dimeric hcAd/AAV.eDYS genomes. Probes 6563 and 2832 are drawn in relation to their target DNA sequences. Numerals correspond to restriction DNA fragment sizes in kilobases.

the dimer-specific 8.4-kb fragments by using probe 2832 alone (Fig. 2B, lane 15), whereas, as expected, the 8.6-kb internal dystrophin DNA-specific segments were detected with probe 6563 (Fig. 2B, lane 13). Interestingly, although less prominent than those corresponding to hcAd.eDYS monomeric replicative forms, DNA fragments consistent with hybrid Ad/AAV.eDYS monomers (Fig. 2C) were also detected (Fig. 2B, compare the 3′ end-specific fragments of 4.8 and 4.4 kb in lanes 3 through 6 with those of 4.5 and 4.2 kb in lanes 7 through 12). This interpretation is further supported by the detection of the 4.2 and 4.5 kb segments after hybridizations with the 3′-end-specific probe 2832 but not with probe 6563 (Fig. 2B, compare lanes 15 and 16 with lanes 13 and 14, respectively).

To determine whether intermolecular recombination via the palindromic AAV ITRs contributes to the generation of the tail-to-tail DNA structures, PER.tTA.Cre76 cells were transfected with equal amounts of pAd/AAV.DsRed and pAd/AAV.EGFP (Fig. 3A, left panel). Control experiments were performed with equimolar mixtures of pAd.DsRed and pAd.EGFP (Fig. 3A, right panel). All constructs were digested with MssI prior to transfection. Direct fluorescence microscopy at ~20 h posttransfection revealed that the large majority of PER.tTA.Cre cells were positive for both marker proteins demonstrating the simultaneous presence of DsRed- and EGFP-encoding plasmids within these cells (Fig. 3B). After infection with Ad.floxedΨ and development of CPE, the producer cell cultures were harvested, and one-tenth of the resulting cleared lysates was added together with Ad.floxedΨ to newly seeded PER.tTA.Cre76 cells. One day later, the cell layers were screened for DsRed- and EGFP-labeled cells by direct fluorescence microscopy (Fig. 3C). As shown above, under the same experimental conditions, we observed tail-to-tail dimers by using hcAd/AAV hybrid vector DNA-encoding plasmids (Fig. 2B, lanes 8, 10, 12, 15, and 16), whereas in control experiments with conventional hcAd vector shuttle constructs monomers were the only structure detected (Fig. 2B, lanes 4 and 6). Hence, transfection of PER.tTA.Cre76 cells with a mixture of MssI-digested pAd.DsRed and pAd.EGFP in the presence of Ad.floxedΨ is not expected to originate hcAd particles that can transfer both reporter genes (Fig. 3A, right panel). AAV ITR-mediated intermolecular recombination between Ad/AAV chimeric genomes would, in addition to homodimers expressing one of the two reporter genes, yield heterodimers encoding both DsRed and EGFP (Fig. 3A, left panel). The results from three independent rescue/assembly and propagation experiments revealed that DsRed- and EGFP-positive cells were rare (Fig. 3C, left panel). Similar results were obtained in the control experiments (Fig. 3C, right panel), indicating that cells colabeled with DsRed and EGFP are, most likely, the result of two independent transduction events of a single cell instead of being caused by the transfer of packaged heterodimers. Taken together, these data suggest that heterodimerization through intermolecular recombination at the AAV ITRs does not play a significant role in the assembly of the tail-to-tail hcAd/AAV chimeric genomes.

In conclusion, the combination of 5′Ad with 3′AAV ITRs in the pAd/AAV shuttle constructs couples Ad DNA-dependent replication to AAV ITR-dependent dimerization, leading to the assembly, in producer cells, of dual hcAd/AAV chimeric genomes with a tail-to-tail genomic organization. Thus, the AAV ITR can be used by the heterologous Ad DNA replication machinery to generate dimeric Ad replicons with a defined structure.

Propagation and quantification of dual hcAd/AAV hybrid vector particles. Subsequently, we determined whether, after assembly, dual hcAd/AAV.eDYS vector particles could be efficiently amplified by serial propagation. To this end, PER.tTA.Cre76 cells were transfected with MssI-digested pAd/AAV.eDYS, infected with Ad.floxedΨ and incubated until CPE was observed. The cell cultures corresponding to this initial rescue/assembly step (P0) were harvested, and one-tenth of the cleared lysates was added to newly seeded PER.tTA.Cre76 cells, together with Ad.floxedΨ at an MOI of 2 IU/cell (passage P1). This infection scheme was repeated in subsequent passages (i.e., passages P2 through P4), except for the use of increasing producer cell numbers. Due to the N-terminal tagging of dystrophin with EGFP, the amplification of dystrophin-coding vector particles could be readily monitored in producer cells both via direct fluorescence microscopy (not shown) and through flow cytometry (Fig. 4). The results from three independent rescue/assembly and propagation experiments initiated with MssI-treated pAd/AAV.eDYS revealed the efficient amplification of dual hcAd/AAV.eDYS hybrid vector particles with the percentage of EGFP-dystrophin-positive producer cells increasing from 3.3 ± 0.46 at P1 to 92.0 ± 1.26 at P4 (Fig. 4). Control rescue/assembly experiments with undigested pAd/AAV.eDYS yielded very few PER.tTA.Cre76 EGFP-dystrophin-positive cells, indicating the necessity to release the Ad/AAV chimeric genomes from the covalently attached prokaryotic DNA to achieve efficient generation of dual hcAd/AAV hybrid vector particles. This finding is in accordance with previous experiments with Ad mini-replicons (22).

Clarified cell lysates obtained after three rounds of vector propagation were purified through CsCl ultracentrifugation. Next, the functional titers of purified hybrid vector preparations were determined by two different methods. The first method quantified the *EGFP-dystrophin* gene transfer activity present in dual hcAd/AAV hybrid vector stocks by endpoint titrations on HeLa indicator cells by using flow cytometry (Table 1). The second procedure consisted of endpoint titrations on PER.tTA.Cre76 cells rendered permissive for dual hcAd/AAV hybrid vector DNA replication via helper Ad.floxedΨ infection. This scheme compensates for the dim fluorescence of the EGFP-dystrophin fusion protein by amplification of the EGFP-dystrophin fluorescence signal in transduced indicator cells. The replication-based assays were designed for higher sensitivity and thus best approximate the number of *EGFP-dystrophin* transducing particles in hybrid vector stocks. In these titration experiments, gene transfer activities were quantified by flow cytometry and by direct fluorescence microscopy (Table 1).

In the direct fluorescence assay, the spread of the EGFP-dystrophin signal via de novo-assembled vector particles was prevented by an agar overlay. Under these conditions, the EGFP-dystrophin-specific fluorescence was limited to individual indicator cells at 20 h p.i. (Fig. 5A). With the progression of the replicative cycle, the EGFP-dystrophin-positive single cells, as expected, developed into fluorescent foci detected by direct fluorescence microscopy at 5 days p.i. (Fig. 5B). Quantification of these foci revealed that their numbers were only

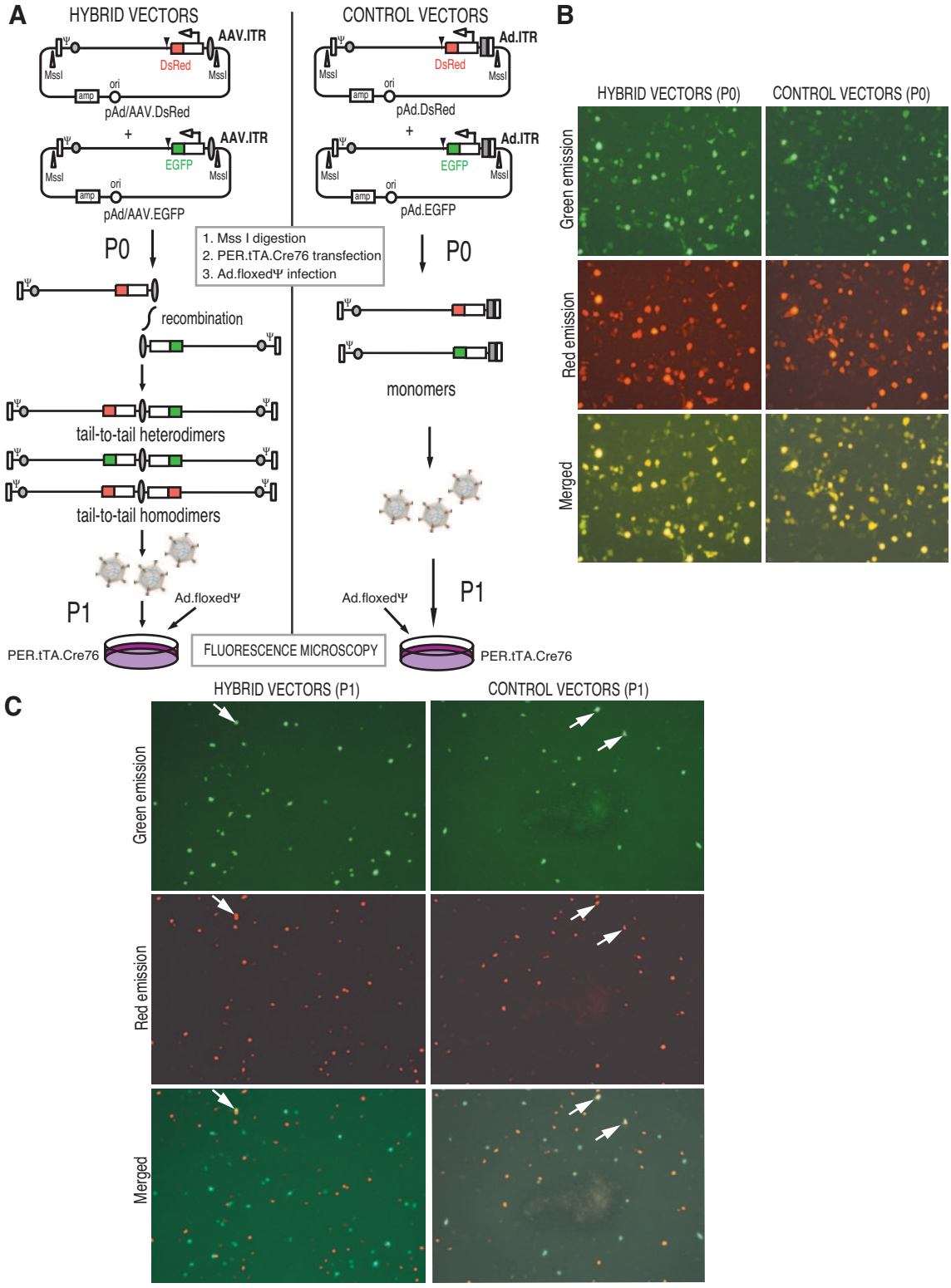

FIG. 3. (A) Experimental set up to test for AAV ITR-mediated intermolecular recombination. (B) Direct fluorescence microscopy analyses on PER.tTA.Cre76 cells transfected either with pAd/AAV.DsRed and pAd/AAV.EGFP (hybrid vectors, P0) or with pAd.DsRed and pAd.EGFP (control vectors, P0). All constructs were digested with MssI prior to transfection. Constructs pAd/AAV.EGFP and pAd.EGFP have exactly the same genetic constitution as pAd/AAV.DsRed and pAd.DsRed, respectively, except that they contain an expression unit consisting of the *EGFP* ORF, followed by the human growth hormone gene pA instead of the *DsRed* ORF linked to an SV40 transcriptional terminator. For a detailed explanation of the genetic elements present in each of the depicted shuttle plasmids, see the legend of Fig. 1A. (C) Representative fluorescence fields of three independent propagation experiments following the set up depicted in panel A on PER.tTA.Cre76 cells at 24 h p.i. Ad.floxedΨ-infected PER.tTA.Cre76 cells received either one-tenth of a cleared cell lysate from pAd/AAV.DsRed- and pAd/AAV.EGFP-transfected and Ad.floxedΨ-infected PER.tTA.Cre76 cells (hybrid vectors, P1) or one-tenth of a cleared cell lysate from pAd.DsRed- and pAd.EGFP-transfected and Ad.floxedΨ-infected PER.tTA.Cre76 cells (control vectors, P1). Arrows indicate cells that are colabeled with EGFP and DsRed.

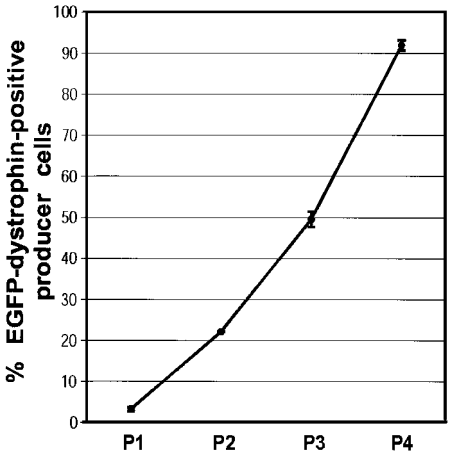

FIG. 4. Serial propagation of dual hcAd/AAV hybrid vector particles on PER.tTA.Cre76 cells. Dual hcAd/AAV.eDYS hybrid vector particles were generated in PER.tTA.Cre76 cells after transfection of MssI-digested pAd/AAV.eDYS, followed by infection with Ad.floxedΨ. Serial propagations (P1, P2, P3, and P4) of hybrid vector particles were performed by inoculating PER.tTA.Cre76 producer cells with one-tenth of clarified cell lysates from the previous passages and Ad.floxedΨ at an MOI of 2 IU/cell. Amplifications of hybrid vector particles encoding the EGFP-dystrophin protein ($n = 3$) were monitored at 24 h p.i. by fluorescence-activated flow cytometry.

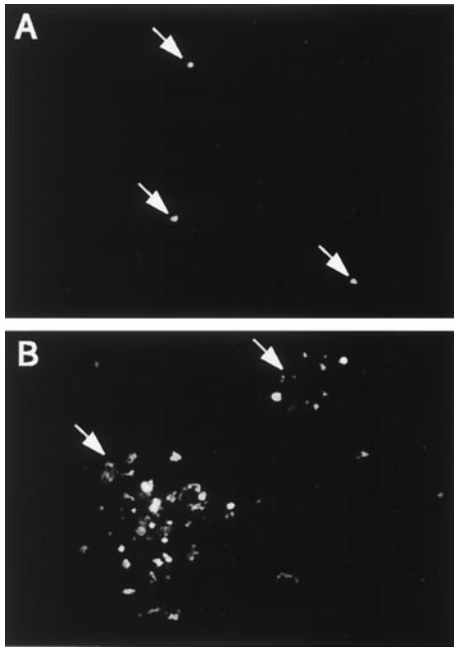

FIG. 5. Representative fluorescence fields of Ad.floxedΨ-infected PER.tTA.Cre76 cells under an agarose overlay at 20 (A) and 120 (B) h after addition of a 10^7-fold dilution of a purified dual hcAd/AAV.eDYS hybrid vector stock. Arrows indicate isolated (A) and clustered (B) EGFP-dystrophin-positive cells.

slightly higher than those of the EGFP-dystrophin-positive single cells, suggesting that this replication-based assay permits accurate determination of gene transfer activities of dual hcAd/AAV.eDYS hybrid vector stocks at 20 h p.i. The titers obtained by direct fluorescence microscopy were on average threefold lower than those measured at 20 h p.i. by fluorescence-activated flow cytometry of indicator cells that had not been covered with agar (compare the values in the fourth column with those in the third column). This difference cannot be attributed to secondary hits since no evidence for spread of the EGFP-dystrophin signal was observed by direct fluorescence microscopy after an incubation period of 20 h. Regardless of the titration assay used, one can conclude that dual hcAd/AAV.eDYS hybrid vector particles are relatively easy to produce and can be concentrated to high titers.

Structure of dual hcAd/AAV hybrid vector genomes. To investigate the structural organization of packaged Ad/AAV chimeric genomes, DNA was extracted from purified hybrid vector particles. Next, the recovered DNA was digested with HincII, BamHI or EcoRV and subjected to Southern blot analysis with a mixture of two vector-specific probes. The results shown in the autoradiogram of Fig. 6A are consistent exclusively with a tandem tail-to-tail genomic organization for packaged Ad/AAV hybrid vector DNA (Fig. 6B), demonstrating that the earlier identified tail-to-tail replicative forms (Fig. 2B, lanes 8, 10, 12, 15, and 16, and Fig. 2C) are packaging-competent substrates. Importantly, no aberrant DNA forms or any other genomic arrangements such as head-to-head or head-to-tail dimers were identified. Interestingly, DNA fragments corresponding to monomeric genomes, previously detected in producer cells during the first round of propagation of hybrid vector particles, were not packaged (compare Fig. 2B, lanes 7, 9, and 15, with Fig. 6A, lane B, and compare Fig. 2B, lanes 8, 10, and 16, with Fig. 6A, lane E).

TABLE 1. Gene transfer activities of dual hcAd/AAV.eDYS hybrid vector stocks as determined by flow cytometry (FC) on HeLa cells at 48 h p.i. and on Ad.floxedψ-infected PER.tTA.Cre76 cells at 20 h p.i. and by direct fluorescence microscopy (DFM) on Ad.floxedψ-infected PER.tTA.Cre76 cells under agarose layers at 20 and 120 h p.i. (hpi)

Stock	Gene transfer activity as determined by:			
	FC		DFM	
	HTU[a]/ml at 48 hpi	FFU/ml at 20 hpi	FFU/ml at 20 hpi	FFU/ml at 120 hpi
1	5.5×10^7	3.0×10^9	8.8×10^8	1.3×10^9
2	2.3×10^7	1.4×10^9	5.4×10^8	0.6×10^9

[a] HTU, HeLa cell-transducing units.

Transfer of the human full-length dystrophin-coding sequence to primary rat cardiomyocytes in vitro by dual hcAd/AAV.eDYS hybrid vectors. A total of 95% of DMD-affected individuals develop heart muscle damage, and 10 to 15% of them die due to cardiac failure (8). The hearts of these patients are damaged by mechanical forces due to the absence of functional dystrophin in cardiomyocytes (9). Heart muscle cells are renowned for being refractory to most gene delivery protocols. However, E1-deleted Ad vectors have been shown to transduce primary cardiomyocytes in vitro, as well as in vivo (20). Thus, we decided to test whether we could deliver the human full-length *DMD* ORF into cardiac cells by dual hcAd/AAV.eDYS hybrid vector transduction. To this end, an in vitro model based on cultures of spontaneously contracting neonatal rat cardiomyocytes was used. These cultures were either mock

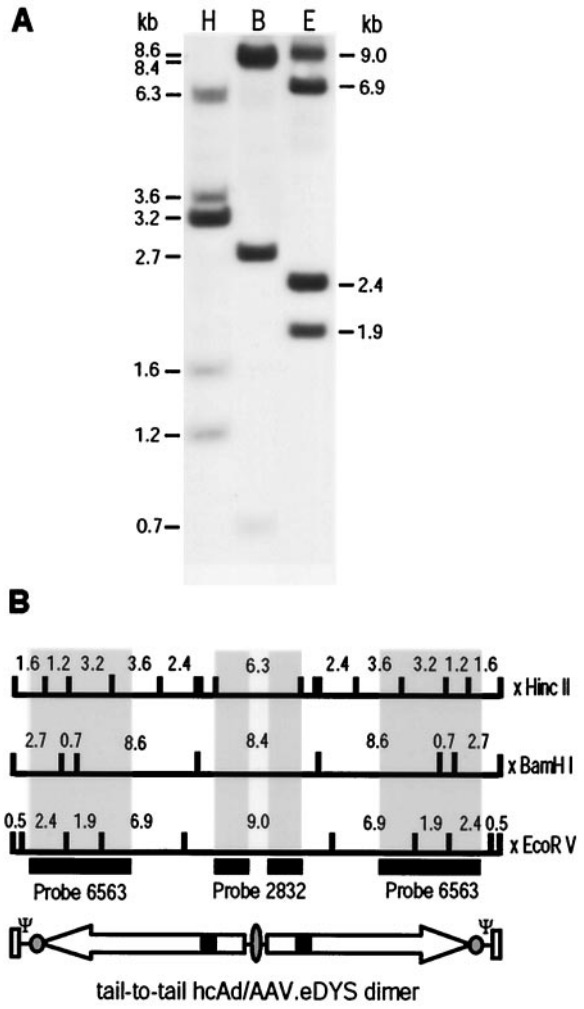

FIG. 6. (A) Structural characterization of packaged dual hcAd/AAV.eDYS hybrid vector DNA. Purified hybrid vector particles obtained after three rounds of propagation on Ad.floxedΨ-infected PER.tTA.Cre76 producer cells were subjected to DNase I treatment, proteinase K digestion, and DNA purification. The purified DNA was digested with HincII (H), BamHI (B) or EcoRV (E). After agarose gel electrophoresis, the resolved DNA fragments were subjected to Southern blotting and DNA hybridizations with a mixture of probes 6563 and 2832. (B) HincII, BamHI, and EcoRV restriction maps of the dimeric hcAd/AAV hybrid vector DNA with a tail-to-tail genomic organization. Solid bars represent DNA probes 6563 and 2832 drawn in relation to their target DNA sequences. Numerals correspond to restriction DNA fragment sizes in kilobases.

transduced or transduced with 10^3 FFU of dual hcAd/AAV.eDYS hybrid vector/cell and, 2 days p.i., direct fluorescence microscopy and immunofluorescence microscopy were used to detect the EGFP-dystrophin and cTNI proteins, respectively. Primary rat cardiomyocyte cultures transduced with an Ad vector with the E1 deleted and encoding EGFP served as a control. Another control consisted of HeLa cells transduced with dual hcAd/AAV.eDYS hybrid vector particles. Vectors based on Ad5 transduce these human cells very well. Bright-field and direct EGFP-dystrophin fluorescence showed the presence of the fusion protein in >90% of the HeLa cells (Fig. 7A and B) and in 70 to 80% of the heart cells (Fig. 7C and D). The immunoreactivity of cells for the cardiac-specific marker cTNI (Fig. 7F, H, J, L, and N) and their rhythmic contraction, which continued after transduction (not shown), confirmed that a significant fraction of the cells in these cultures is indeed cardiomyocytes. Moreover, the characteristic striated banding pattern of cTNI in cardiac muscle cells was discerned (Fig. 7J). The detection of the EGFP-dystrophin protein (Fig. 7E and G) in the large majority of cTNI-positive cells (Fig. 7F and H) indicates efficient transduction of cardiomyocytes by dual hcAd/AAV.eDYS hybrid vector particles. Finally, comparison of the intracellular distribution of EGFP versus that of EGFP-dystrophin showed that, while the former pervaded the entire cell, including the nucleus (Fig. 7K), the latter was excluded from nuclei and was found associated with the plasmalemma of cardiomyocytes (Fig. 7G and I). These results are in agreement with the known intracellular localization of the wild-type dystrophin protein and with data retrieved from experiments with this *EGFP-dystrophin* gene in the context of nonviral DNA transfections (6). Finally, mock-transduced cells did not exhibit green fluorescence, showing that this signal was specific for the presence of EGFP in vector-transduced cells (Fig. 7M and N).

Transfer of the human full-length dystrophin-coding sequence to dystrophic mouse skeletal muscle in vivo by dual hcAd/AAV.eDYS hybrid vectors. The underlying genetic cause of the dystrophic phenotype of *mdx* mice lies in a premature stop codon in exon 23 of dystrophin (47). With the exception of rare so-called revertant muscle fibers, no dystrophin protein is observed in muscle tissue of *mdx* mice. The skeletal muscle of adult *mdx* mice displays certain histopathologic features characteristic of DMD, such as heterogeneity in muscle fiber diameter and a high prevalence of centrally located nuclei. These attributes make *mdx* mice an attractive model system for evaluating procedures aimed at the rescue of dystrophin synthesis, particularly at the histological level.

To investigate the in vivo efficacy of dual hcAd/AAV hybrid vector-mediated gene delivery, we injected the gastrocnemius muscles of three adult, 6-week-old, *mdx* mice with 2×10^8 FFU of dual hcAd/AAV.eDYS hybrid vector. Negative controls consisted of *mdx* gastrocnemius muscles sham injected with buffer solution only, whereas dystrophin-positive gastrocnemius muscles from syngeneic wild-type mice were included as positive controls. At 6 days postinjection, muscle sections from each of the experimental groups were subjected to immunohistochemistry by using an MAb directed against the C-terminal portion of the dystrophin protein. Immunohistochemical analyses of positive control specimens derived from wild-type mice exhibited sarcolemmal staining in uniformly sized muscle fibers with peripheral nuclei (Fig. 8A), whereas those of sham-injected muscles did not reveal dystrophin-positive fibers (Fig. 8B). The results obtained with the positive and negative control samples attest to the specificity of the immunohistochemical assay for the dystrophin protein. Analyses of cross sections derived from dual hcAd/AAV.eDYS hybrid vector-injected *mdx* muscles revealed clear and widespread recombinant full-length *dystrophin* expression (Fig. 8C to F). The dystrophin protein localized properly to the sarcolemma of dystrophic muscle fibers characterized, as mentioned above, by a broad range of cross section sizes and central nucleation (Fig. 8C and D). In addition to the strong labeling of the sarcolemma, some

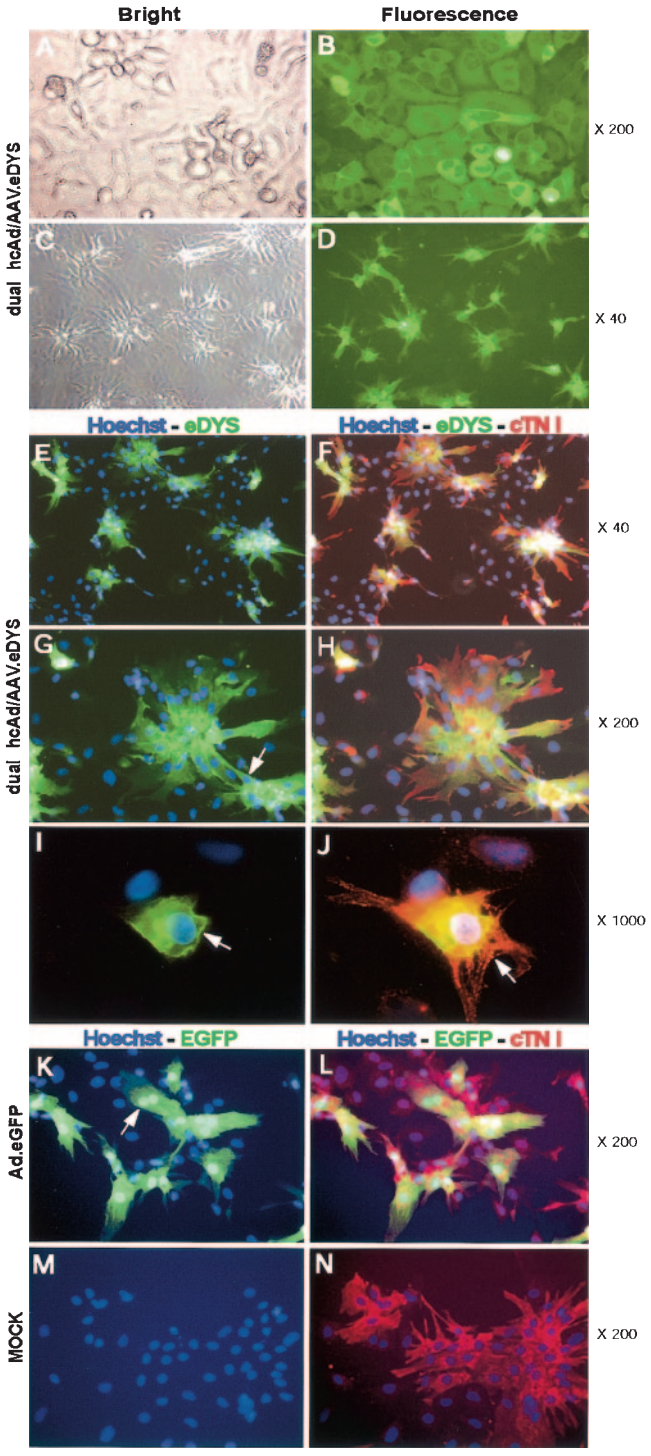

FIG. 7. Direct fluorescence microscopy and immunofluorescence microscopy of rat primary cardiomyocyte cultures transduced with dual hcAd/AAV.eDYS hybrid vector particles. (A and B) Bright-field (A) and equivalent fluorescence field (B) images of HeLa cell cultures transduced with dual hcAd/AAV.eDYS hybrid vector particles at an MOI of 2×10^2 FFU/cell. (C and D) Bright-field (C) and equivalent fluorescence field (D) images of rat primary cardiomyocyte cultures transduced with dual hcAd/AAV.eDYS hybrid vector particles at an MOI of 10^3 FFU/cell. (E, G, I, K, and M) Direct fluorescence microscopy of cardiomyocyte cultures mock-transduced (M) or transduced either with 10^3 FFU/cell of dual hcAd/AAV.eDYS hybrid vector (E, G, and I) or with 10^2 IU/cell of the control vector Ad.ΔE1.EGFP (K). Nuclei were visualized through Hoechst 33342 staining (blue), and the corresponding signal was merged with the EGFP-specific fluorescence (green). The arrows in panels G and I indicate cells in which the EGFP-dystrophin signal is excluded from the nucleus, whereas the arrow in panel K points to a cell in which the nonfusion protein EGFP has permeated the nuclei. The arrow in panel I indicates, in addition, the localization of part of the EGFP-dystrophin staining to the plasma membrane of the cardiomyocyte. (F, H, J, L, and N) cTNI immunofluorescence microscopy and direct fluorescence microscopy of rat heart cell cultures mock transduced (N) or transduced either with 10^3 FFU/cell of dual hcAd/AAV.eDYS hybrid vector (F, H, and J) or with 10^2 IU/cell of the control vector Ad.ΔE1.EGFP (L). Cardiomyocytes were labeled with a Cy3-conjugated cTNI-specific MAb (red), and the resultant staining pattern was merged with both the EGFP and Hoechst 33342 signals. The arrow in panel J points to a region of a cardiomyocyte with a striated distribution pattern of the cardiac-specific protein cTNI. All microscopic analyses were performed at 48 h p.i.

fibers also revealed detectable cytoplasmic staining indicative of transgene overexpression (Fig. 8E). Taken together, these experiments demonstrate the ability of dual hcAd/AAV.eDYS hybrid vectors to efficiently deliver and express the full-length human dystrophin-coding sequence in cardiomyocytes in vitro as well as in adult dystrophic skeletal muscle in vivo.

Targeted DNA integration after dual hcAd/AAV hybrid vector-mediated gene delivery. Finally, we investigated whether introduction of dual hcAd/AAV chimeric genomes into human cells provided with the AAV Rep78 and Rep68 proteins could lead to *AAVS1*-targeted DNA integration. To this end, HeLa cells were transfected either with expression plasmid pGAP-DH.Rep78/68 encoding AAV Rep78 and Rep68 or with expression plasmid pKS.P5.Rep coding for Rep78, Rep68, Rep52, and Rep40. Control experiments consisted of mock-transfected HeLa cells and of HeLa cells transfected with plasmid pEFO.DsRed.T4 containing a *DsRed* ORF in place of AAV *rep*. Next, the cells were transduced with dual hcAd/AAV.eDYS hybrid vector particles at three different MOIs. At 3 days p.i., genomic DNA was extracted from these cells and a PCR-based DNA integration assay was performed to detect *AAVS1*-hybrid vector DNA junctions using two primer sets (Fig. 9A). These primers anneal to the hybrid vector genome and to the chromosome 19 region where AAV DNA insertions have been mapped (30, 32, 43). PCR-amplified samples were subjected to agarose gel electrophoresis and Southern blot hybridizations with either a hybrid vector- or an *AAVS1*-specific probe (Fig. 9B, upper and lower panels, respectively). In both instances, a collection of differently sized DNA fragments migrating as a smear was observed in samples of AAV *rep*-transfected and dual hcAd/AAV.eDYS-infected cells (Fig. 9B, lanes 3 through 5, 7, and 8). Samples derived from HeLa cells that were transduced with dual hcAd/AAV hybrid vector particles after being either mock- or pEFO.DsRed.T4-transfected (Fig. 9B, lanes 1 and 2, respectively) did not yield hybridization signals. These results demonstrate AAV Rep-dependent targeted integration of hybrid vector DNA into *AAVS1*. AAV DNA integration events are not site specific in a classic sense since they do not take place at a single nucleotide position but within a relatively long stretch of DNA. Consequently, *AAVS1*-hybrid vector DNA junctions generated through the AAV DNA integration process are usually present as single copies within the population of *AAVS1*-targeted cells. Therefore, the

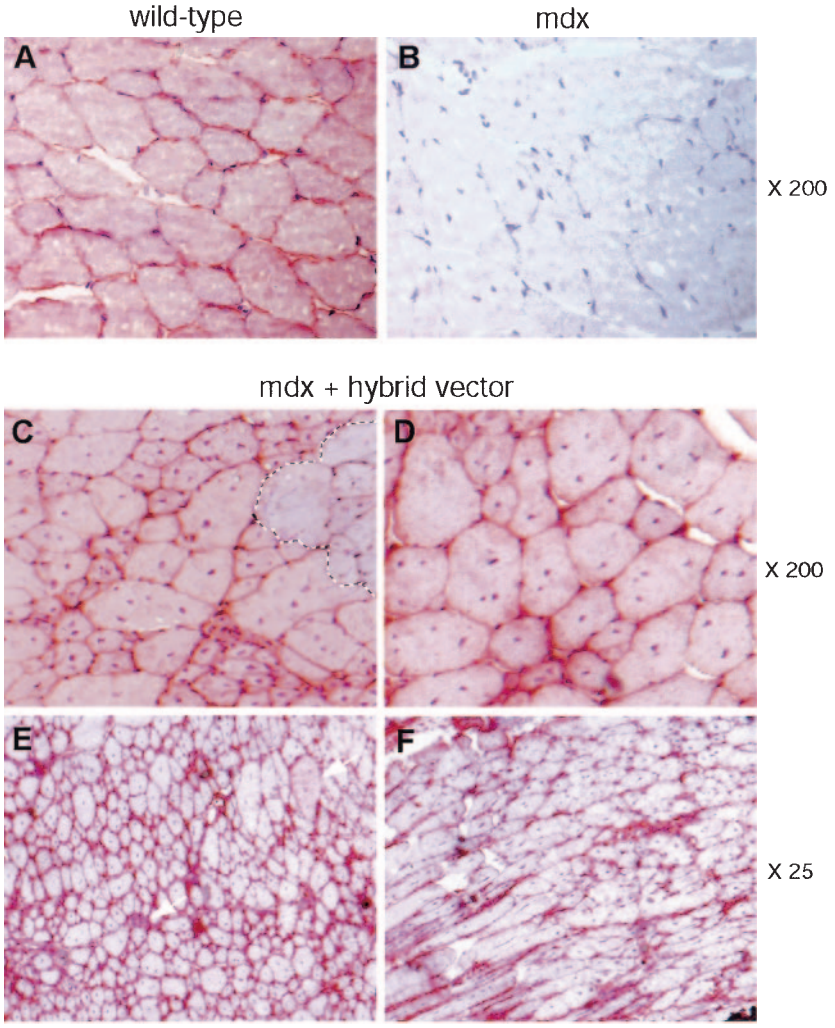

FIG. 8. Immunohistochemical staining of *mdx* skeletal muscles following direct injection of dual hcAd/AAV.eDYS hybrid vector particles. Immunohistochemical staining with a MAb directed against the C terminus of the human dystrophin protein of gastrocnemius muscles from wild-type (A) and sham-injected dystrophin-deficient *mdx* (B) mice and of *mdx* mice injected with 2×10^8 FFU of dual hcAd/AAV.eDYS hybrid vector FFU (C, D, E, and F). The dashed line in panel C delimits an area of dystrophin-negative *mdx* myofibers. The arrows in panel E point to myofibers with cytoplasmic staining.

observed smear most likely reflects the amplification of a mixture of *AAVS1*-hybrid vector DNA junctions with various lengths. To investigate this, the PCR products were cloned into the cloning vector pCR4-TOPO. Recombinant plasmids from randomly selected colonies were digested with EcoRI to release the inserts. Analyses by agarose gel electrophoresis showed inserts with different sizes mirroring the diversity of DNA fragment sizes observed in Fig. 9B (Fig. 9C, upper panel). To further confirm the nature of these inserts as being *AAVS1*-hybrid vector DNA junctions, the DNA samples were transferred in duplicate to blotting membranes and incubated separately with the probes depicted in Fig. 9A. After autoradiography, both the hybrid vector- and the *AAVS1*-specific probes recognized all clones analyzed (Fig. 9C, middle and lower panels, respectively), corroborating that they represent junctions between the AAV preintegration site on chromosome 19 and hybrid vector DNA. The inserts of clones L13, H1, and H8 (Fig. 9C, middle panel) and 8 (Fig. 9C, lower panel) were clearly detected upon extension of the exposure time in the absence of any other hybridization signals (not shown). Interestingly, for both probes the signal strengths varied between different clones (Fig. 9C, middle and lower panels). In addition, most clones reacted to a different extent with the two probes (Fig. 9C, compare the middle and lower panels). These results indicate the existence of clone-specific truncations not only within the *AAVS1* region but also within the hybrid vector DNA affecting, to different extents, probe annealing. Therefore, to study in fine detail the structure of the *AAVS1*-hybrid vector DNA junctions, nucleotide sequence analyses were performed on clones 3, 5, 7, L2, and H10. The results summarized in Fig. 10A confirmed host chromosomal DNA breakpoints scattered throughout the *AAVS1* region downstream of the trs and Rep-binding element (RBE; Fig. 10B). Moreover, the hybrid vector DNA was always broken upstream of the RBE in the p5IEE sequence (Fig. 10C). These data confirm that each insert has a specific sequence. More-

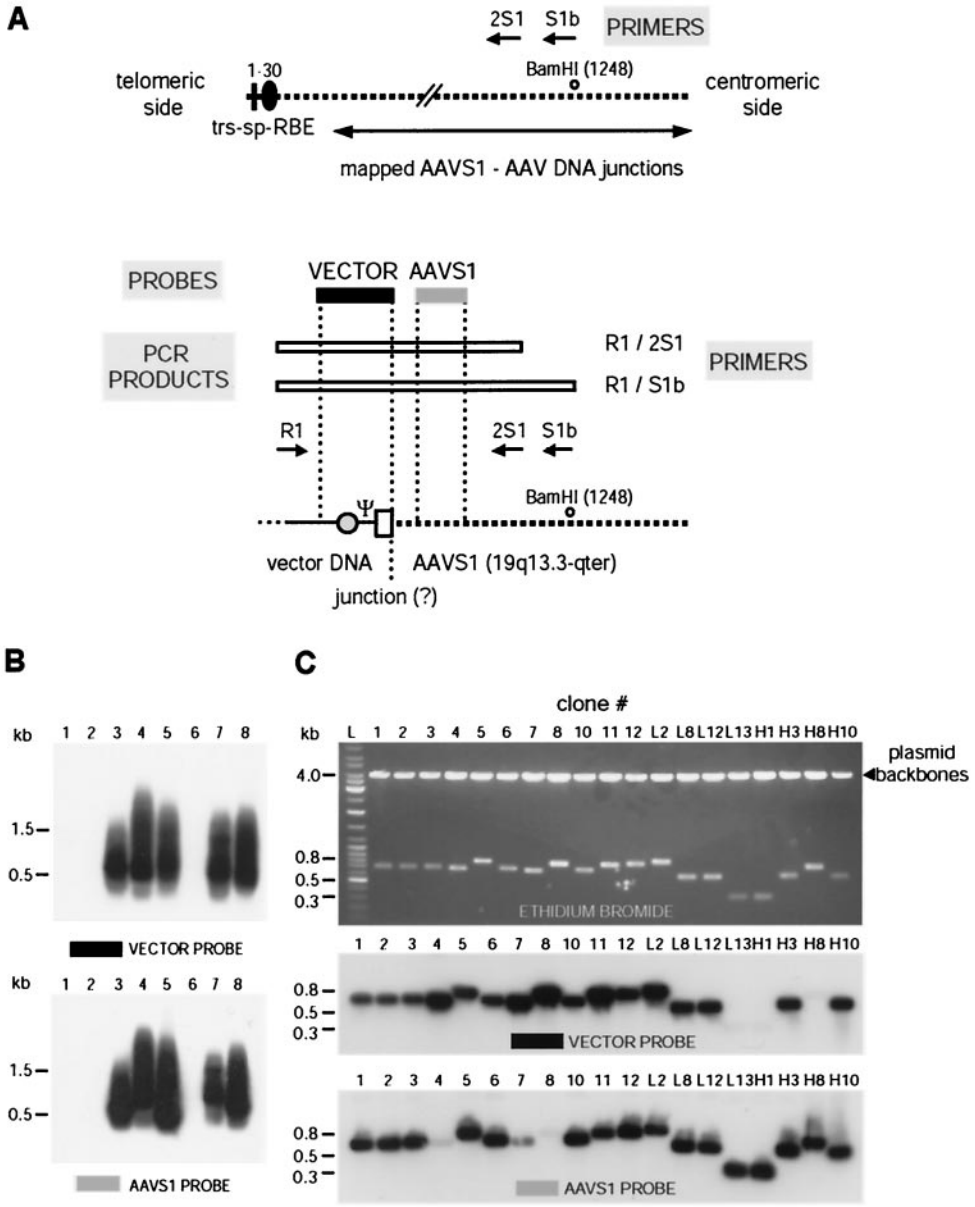

FIG. 9. Site-specific integration of foreign DNA into *AAVS1* after gene transfer with dual hcAd/AAV.eDYS hybrid vectors. (A) Illustration of the targeted DNA integration assay with the primers used (arrows) drawn in relation to their respective target DNA templates. The upper panel shows a section of human chromosome 19 at 19q13.3-qter with *AAVS1* sequences (dotted line). The beginning of this DNA region was set arbitrarily at the first nucleotide position of the previously defined trs (32). Numeral 30 corresponds to the position of the last nucleotide of the RBE. Vertical line and solid oval, trs and RBE, respectively, separated by a spacer sequence (sp); double-headed arrow, AAV DNA preintegration region; open circle, BamHI recognition site located 1,248 nucleotides downstream of the trs-sp-RBE sequence. The lower panel is a schematic representation of a targeted DNA integration event leading to an *AAVS1*-hybrid vector DNA junction. Shaded circle, AAV p5IEE; Ψ, Ad packaging signal-containing sequence; open box, Ad ITR; open bars, PCR products obtained with the primer combinations Beta.R1 (R1) plus pAAVS1b (S1b) and Beta.R1 (R1) plus Cr2-AAVS1 (2S1); solid bar, hybrid vector-specific probe; shaded bar, *AAVS1*-specific probe. (B) Southern blot hybridizations with hybrid vector- and *AAVS1*-specific probes (upper and lower panel, respectively) of PCR-amplified DNA obtained with the set up depicted in panel A using genomic DNA extracted from HeLa cells that were either mock transfected (lanes 1) or transfected with pEFO.DsRed.T4 (lanes 2), pGAPDH.Rep78/68 (lanes 3 through 5), or pKS.P5.Rep (lanes 7 and 8). Lanes 6 correspond to the GeneRuler DNA Ladder Mix molecular weight marker. Three days before chromosomal DNA extraction, transfected and mock-transfected HeLa cells were transduced with dual hcAd/AAV.eDYS hybrid vector particles at 18 (lanes 3 and 7), 90 (lanes 4) and 450 FFU/cell (lanes 1, 2, 5, and 8). (C) Agarose gel electrophoreses (upper panel) and Southern blot hybridizations with hybrid vector- and *AAVS1*-specific probes (middle and lower panel, respectively) of cloned PCR products obtained after amplification on genomic DNA extracted from HeLa cells that were transfected with pGAPDH.Rep78/68 and subsequently transduced with dual hcAd/AAV.eDYS hybrid vectors at an MOI of 90 FFU/cell. Recombinant DNA plasmids isolated from randomly selected colonies were, prior to agarose gel electrophoresis, digested with EcoRI to release the inserts from the plasmid backbones.

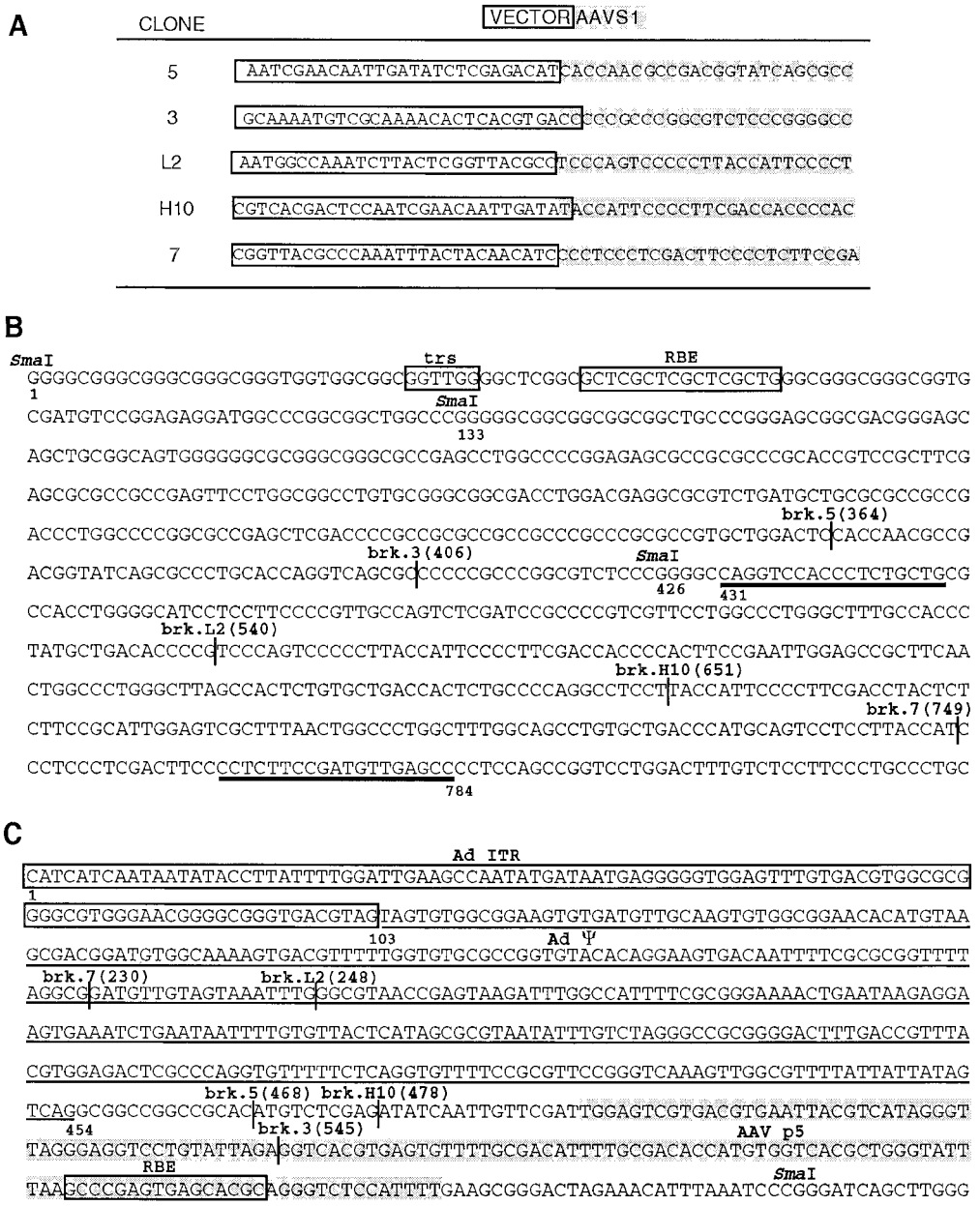

FIG. 10. (A) Junctions between dual hcAd/AAV.eDYS hybrid vector DNA and human chromosome 19. Hybrid vector DNA is boxed and *AAVS1* sequences are shaded. (B) Breakpoints within *AAVS1* after hybrid vector gene transfer into AAV pKS.P5.Rep-transfected cells. Open boxes, trs and RBE; vertical lines, location of breakpoints (brk.); horizontal lines, binding sites of the primers used to PCR amplify the *AAVS1*-specific probe. (C) Breakpoints within dual hcAd/AAV.eDYS chimeric genomes after dual hcAd/AAV.eDYS hybrid vector gene transfer into AAV pKS.P5.Rep-transfected cells. Open box, Ad ITR sequence; horizontal line, Ad packaging signal-containing sequence; shaded nucleotides, AAV p5IEE; shaded box, RBE.

over, the analyzed junctions did not contain sequences other than those of the hybrid vector genome and *AAVS1*. Finally, the intensities of the Southern blot hybridization signals are consistent with the DNA sequence data. For instance, the inserts of clones 3 and 7, which display the weakest hybridization signals with the vector- and chromosome 19-specific probes, respectively, have the shortest sequence overlap with these probes. Altogether, these experiments demonstrate the ability of dual hcAd/AAV hybrid vectors to target foreign DNA into the *AAVS1* locus on human chromosome 19 provided that the Rep78 and Rep68 proteins are available within transduced cells.

DISCUSSION

hcAd vectors achieve efficient transfer of the full-length *DMD* cDNA in vitro and in vivo (19, 27, 31) and, due to the lack of Ad protein-coding sequences, are noticeably less immunogenic than Ad vectors with one (i.e., first-generation) or more (i.e., second-generation) early regions deleted (28).

Nonetheless, if large amounts of Ad capsids are used in vivo, they can still trigger an acute inflammatory reaction (5, 49). Therefore, increasing the number of therapeutic gene copies delivered within each Ad capsid will allow the use of lower vector doses to attain a certain transgene expression level. In addition, conventional hcAd vectors are not suited for the permanent genetic correction of proliferating cell populations because the delivered DNA normally remains episomal. In the present study, a new gene transfer system that builds on the attractive features of hcAd vectors is presented. These dual hcAd/AAV hybrid vectors carry dimeric genomes and can stably transduce target cells by DNA integration into a predefined site within the human DNA.

Here, we have shown that the Ad DNA replication machinery can be coupled to the AAV ITR-mediated dimerization process to assemble defined Ad DNA replicons in helper Ad vector-infected E1-complementing producer cells. By applying this principle we produced hybrid vector particles encoding two full-length human dystrophin-coding sequences. We postulate two pathways for the initial rescue and replication of dual hcAd/AAV hybrid vectors (Fig. 11). After transfection of MssI-digested Ad/AAV hybrid vector shuttle plasmids into PER.tTA.Cre76 cells, the producer cells are infected with the E1-deleted helper Ad vector Ad.floxedΨ. In pathway I, the AAV ITRs are resolved into covalently closed hairpins by the AAV Rep78 and Rep68 proteins or, alternatively, by cellular activities that act on their Holliday-like secondary structure (53, 55). This structure can be formed at the AAV ITR due to its multipalindromic nature. Interestingly, higher packaging levels of Ad/AAV chimeric genomes into Ad capsids were observed in the presence of AAV Rep proteins most likely as a result of the enhanced resolution of the AAV ITRs from the covalently attached prokaryotic DNA by the AAV Rep catalytic activities. These data are in accordance with previous DNA resolution experiments with AAV ITR-containing plasmid substrates in the presence or absence of AAV *rep* expression (55). The Ad DNA replication initiation complex recognizes the Ad ITR located close to the other end of the molecules. Subsequently, strand displacement and DNA polymerization that advances through the covalently closed AAV ITR hairpin structures, follow. These processes generate DNA structures containing at both ends Ad origins of replication and packaging elements, which makes them efficient substrates for Ad DNA-dependent replication and packaging, respectively. Pathway II develops from DNA substrates not resolved through the AAV ITRs and entails the complete strand displacement of parental templates by the Ad DNA replication machinery. For simplicity, the duplex daughter molecules produced during this process are not drawn. The resulting single-stranded DNA molecules contain AAV ITRs with unpaired tails at their 3′ ends. The removal of these tails by 3′ exonucleases generates hairpins with free 3′ hydroxyl groups. These structures constitute ideal primers for DNA polymerization. After elongation, duplex 5′ Ad ITRs with functional Ad DNA origins of replication are regenerated. Next, Ad DNA dependent-reinitiation, followed by DNA polymerization through the AAV ITR hairpin, leads once again to DNA molecules containing at both ends Ad origins of replication and Ad packaging elements. These structures can be further amplified and packaged into Ad capsids. The two pathways described above

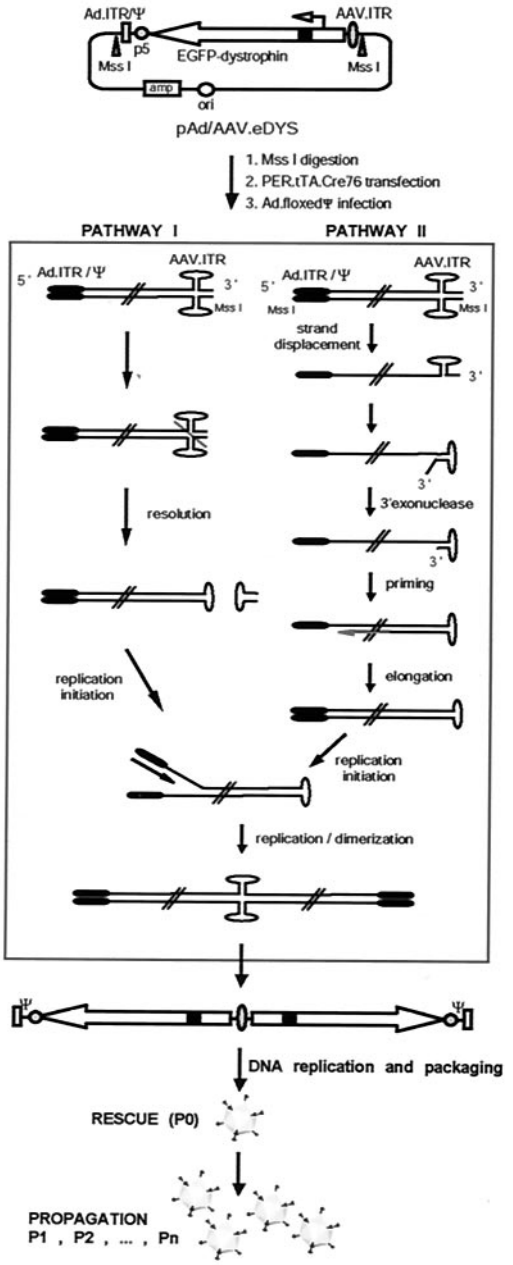

FIG. 11. Diagram for the rescue and replication of dual hcAd/AAV hybrid vectors (see the text for details).

are not mutually exclusive and, in accordance with the experimental data, converge into a single product type (i.e., tail-to-tail dimers).

After assembly, dual hcAd/AAV.eDYS hybrid vector particles could be amplified to high titers through serial propagation on Ad.floxedΨ-infected PER.tTA.Cre76 producer cells. The structural analyses of DNA extracted from dual hcAd/AAV.eDYS hybrid vector particles confirmed packaging of tail-to-tail tandem genomes. Although monomers were not detected within vector particles, they were present in the extrachromosomal DNA fraction of producer cells after one round of propagation. Moreover, they were also found in pro-

ducer cells during second passages (not shown). These data suggest that a fraction of the dual hcAd/AAV chimeric genomes is resolved into monomers possibly due to cellular activities acting on the Holliday-like cruciform structures that can be formed at the centrally localized AAV ITRs (55). Moreover, the absence of monomers from the packaged DNA pool may be related to the preferential encapsidation of dimeric genomes whose length is above the lower genome size limit reported to be necessary for efficient Ad DNA packaging (37).

Fluorescence microscopy data from experiments with the recombinant human dystrophin tagged at the N terminus with EGFP, together with the immunohistochemistry results obtained with a dystrophin C terminus-specific MAb, showed efficient transfer of the recombinant *DMD* gene into muscle cells in vitro and in vivo and synthesis of the full-length dystrophin protein in these cells. Although this protein localized properly to the sarcolemma of dystrophic *mdx* muscle fibers, the redistribution of myofiber nuclei to the periphery of the syncytia was not observed. This result is likely attributable to the fact that the gene transfer procedure took place at adulthood (13) and to the long time span required for this phenomenon to happen.

Previous results have pointed to the involvement of the DNA sequence that overlaps with the p5 promoter in AAV DNA targeted integration because of the high frequency of breakpoints observed within or in the vicinity of this region in addition to the breakpoints that were found inside the AAV ITRs (14, 43, 50). More recently, the direct involvement of this DNA sequence in the high-level site-specific integration of foreign DNA was demonstrated in the context of transfection experiments carried out with circular plasmid molecules (38, 39). The p5IEE is absent from standard recombinant AAV vectors, which contain from the parental virus genome exclusively the AAV ITRs. Introduction of the p5IEE sequence into recombinant AAV vectors, to restore high-level site-specific DNA integration, will further reduce their already limited coding capacity. In the present study, we provided evidence that the efficient Ad capsid-mediated gene transfer process can be utilized to introduce into the nuclei of target cells large DNA segments reminiscent of AAV proviral genomes, and we showed that these structures are substrates for *AAVS1*-targeted DNA integration in the presence of AAV Rep proteins. Nucleotide sequence analyses of *AAVS1*-hybrid vector DNA junctions revealed that the breakpoints occurred upstream of the RBE in p5IEE leaving behind the complete Ad ITR and some or all of the Ad packaging elements. This feature is important for two reasons. First, it suggests that disruption of therapeutic and/or transgenic DNA sequences does not happen frequently and, second, it indicates that the integrated genetic information will not be prone to mobilization after infection of stably transduced cells with a complementing wild-type Ad (40).

Cell- and gene-based approaches to DMD therapy are currently under intense investigation. The former entail the isolation and allogeneic transplantation of progenitor or stem cells with myogenic potential, whereas the latter aim directly at complementing the faulty *DMD* gene through transfer of a functional dystrophin-coding sequence. A third route for the management of DMD would be to combine these two approaches to enable genetic correction and autologous transplantation of the cell type(s) that turn out to have the highest regenerative capacity of the most life-threatening dystrophic muscles. At present, however, there is no gene delivery system that permits the stable transduction of the full-length *DMD* cDNA into proliferating dystrophin-defective myogenic cells.

Dual hcAd/AAV hybrid vectors may become a gene transfer system of choice to bridge the gap between gene- and cell-based approaches for the treatment of DMD, provided that an efficient method to transiently express AAV Rep activities in target cells is developed (e.g., via protein transfer technologies, through incorporation of a conditionally regulated AAV *rep* expression unit into the nonintegrating portion of the hybrid vector DNA or via delivery of AAV *rep* by a second vector particle). The short-term presence of AAV *rep* gene products aims at achieving site-specific integration of foreign DNA while minimizing the potential deleterious effects of these proteins (e.g., cell cycle arrest).

ACKNOWLEDGMENTS

We thank Jacques Tremblay (Human Genetic Research Unit, Laval University Hospital Center, Sainte-Foy, Quebec, Canada), Shuichi Yanagisawa (Department of Life Sciences, Graduate School of Arts and Sciences, The University of Tokyo, Tokyo, Japan), Louis-Marie Houdebine (Unité de Différenciation Cellulaire, Institut National de la Recherche Agronomique, Jouy en Josas, France), Benjamin Glick (Department of Molecular Genetics and Cell Biology, The University of Chicago, Chicago, Ill.), and Jun-ichi Miyazaki (Division of Stem Cell Regulation Research, Osaka University Medical School, Osaka, Japan) for plasmids pDysE, pGAP489CAT, pEFO, pDsRed.T4-N1, and pCAGGS, respectively. We also thank Lizet van der Valk-Kokshoorn and Arnoud van der Laarse (Department of Cardiology, Leiden University Medical Center, Leiden, The Netherlands) for making available cultures of primary rat cardiomyocytes and Ieke Ginjaar (Department of Human and Clinical Genetics, Leiden University Medical Center, Leiden, The Netherlands) for the NCL-DYS2 antibody.

Manuel Gonçalves initiated his Ph.D. at the Department of Molecular Cell Biology of the Leiden University Medical Center with support from the Fundação Portuguesa para a Ciência e Tecnologia (MCT-FCT; Grant Praxis XXI/BD/9157/96). This research was partially supported by the Technology Foundation for Science and Technology STW, the Applied Science Division of NWO, and the Technology Program of the Ministry of Economic Affairs of The Netherlands.

REFERENCES

1. **Aki, T., S. Yanagisawa, and H. Akanuma.** 1997. Identification and characterization of positive regulatory elements in the human glyceraldehyde 3-phosphate dehydrogenase gene promoter. J. Biochem. **122:**271–278.
2. **Bett, A. J., L. Prevec, and F. L. Graham.** 1993. Packaging capacity and stability of human adenovirus type 5 vectors. J. Virol. **67:**5911–5921.
3. **Bevis, B. J., and B. S. Glick.** 2002 Rapidly maturing variants of the *Discosoma* red fluorescent protein (DsRed). Nat. Biotechnol. **20:**83–87.
4. **Blake, D. J., A. Weir, S. E. Newey, and K. E. Davies.** 2002. Function and genetics of dystrophin and dystrophin-related proteins in muscle. Physiol. Rev. **82:**291–329.
5. **Brown, B. D., C. X. Shi, S. Powell, D. Hurlbut, F. L. Graham, and D. Lillicrap.** 2004. Helper-dependent adenoviral vectors mediate therapeutic factor VIII expression for several months with minimal accompanying toxicity in a canine model of severe hemophilia A. Blood **103:**804–810.
6. **Chapdelaine, P., P.-A. Moisset, P. Campeau, I. Asselin, J.-T. Vilquin, and J. P. Tremblay.** 2000. Functional EGFP-dystrophin fusion proteins for gene therapy vector development. Protein Eng. **13:**611–615.
7. **Chiorini, J. A., M. D. Weitzman, R. A. Owens, E. Urcelay, B. Safer, and R. M. Kotin.** 1994. Biologically active rep proteins of adeno-associated virus type 2 produced as fusion proteins in *Escherichia coli*. J. Virol. **68:**797–804.
8. **Cox, G. F., and L. M. Kunkel.** 1997. Dystrophies and heart disease. Curr. Opin. Cardiol. **12:**329–343.
9. **Danialou, G., A. S. Comtois, R. Dudley, G. Karpati, G. Vincent, C. Des Rosiers, and B. J. Petrof.** 2001. Dystrophin-deficient cardiomyocytes are abnormally vulnerable to mechanical stress-induced contractile failure and injury. FASEB J. **15:**1655–1657.

10. **Fallaux, F. J., A. Bout, I. van der Velde, D. J. M. van den Wollenberg, K. M. Hehir, J. Keegan, C. Auger, S. J. Cramer, H. van Ormondt, A. J. van der Eb, D. Valerio, and R. C. Hoeben.** 1998. New helper cells and matched early region 1-deleted adenovirus vectors prevent generation of replication-competent adenoviruses. Hum. Gene Ther. **9:**1909–1917.
11. **Gilbert, R., R. W. R. Dudley, A.-B. Liu, B. J. Petrof, J. Nalbantoglu, and G. Karpati.** 2003. Prolonged dystrophin expression and functional correction of *mdx* mouse muscle following gene transfer with a helper-dependent (gutted) adenovirus-encoding murine dystrophin. Hum. Mol. Genet. **12:**1287–1299.
12. **Gilbert, R., A.-B. Liu, B. J. Petrof, J. Nalbantoglu, and G. Karpati.** 2002. Improved performance of a fully gutted adenovirus vector containing two full-length dystrophin cDNAs regulated by a strong promoter. Mol. Ther. **6:**501–509.
13. **Gilchrist, S. C., M. P. Ontell, S. Kochanek, and P. R. Clemens.** 2002. Immune response to full-length dystrophin delivered to *dmd* muscle by a high-capacity adenoviral vector. Mol. Ther. **6:**359–368.
14. **Giraud, C., E. Winocour, and K. I. Berns.** 1995. Recombinant junctions formed by site-specific integration of adeno-associated virus into an episome. J. Virol. **69:**6917–6924.
15. **Gonçalves, M. A. F. V., M. G. Pau, A. A. F. de Vries, and D. Valerio.** 2001. Generation of a high-capacity hybrid vector: packaging of recombinant adenoassociated virus replicative intermediates in adenovirus capsids overcomes the limited cloning capacity of adenoassociated virus vectors. Virology **288:**236–246.
16. **Gonçalves, M. A. F. V., I. van der Velde, J. M. Janssen, B. T. H. Maassen, E. H. Heemskerk, D.-J. E. Opstelten, S. Knaän-Shanzer, D. Valerio, and A. A. F. de Vries.** 2002. Efficient generation and amplification of high-capacity adeno-associated virus/adenovirus hybrid vectors. J. Virol. **76:**10734–10744.
17. **Gonçalves, M. A. F. V., I. van der Velde, S. Knaän-Shanzer, D. Valerio, and A. A. F. de Vries.** 2004. Stable transduction of large DNA by high-capacity adeno-associated virus/adenovirus hybrid vectors. Virology **321:**287–296.
18. **Greelish, J. P., L. T. Su, E. B. Lankford, J. M. Burkman, H. Chen, S. K. Konig, I. M. Mercier, P. R. Desjardins, M. A. Mitchell, X. G. Zheng, J. Leferovich, G. P. Gao, R. J. Balice-Gordon, J. M. Wilson, and H. H. Stedman.** 1999. Stable restoration of the sarcoglycan complex in dystrophic muscle perfused with histamine and a recombinant adeno-associated viral vector. Nat. Med. **5:**439–443.
19. **Haecker, S. E., H. H. Stedman, R. J. Balice-Gordon, D. B. J. Smith, J. P. Greelish, M. A. Mitchell, A. Wells, H. L. Sweeney, and J. M. Wilson.** 1996. In vivo expression of full-length human dystrophin from adenoviral vectors deleted of all viral genes. Hum. Gene Ther. **7:**1907–1914.
20. **Hajjar, R. J., F. del Monte, T. Matsui, and A. Rosenzweig.** 2000. Prospects for gene therapy for heart failure. Circ. Res. **86:**616–621.
21. **Harper, S. Q., M. A. Hauser, C. DelloRusso, D. Duan, R. W. Crawford, S. F. Phelps, H. A. Harper, A. S. Robinson, J. F. Engelhardt, S. V. Brooks, and J. S. Chamberlain.** 2002. Modular flexibility of dystrophin: implications for gene therapy of Duchenne muscular dystrophy. Nat. Med. **8:**253–261.
22. **Hay, R. T., N. D. Stow, and I. M. McDougall.** 1984. Replication of adenovirus mini-chromosomes. J. Mol. Biol. **175:**493–510.
23. **Hong, G., P. Ward, and K. I. Berns.** 1994. Intermediates of adeno-associated virus DNA replication in vitro. J. Virol. **68:**2011–2015.
24. **Hüser, D., and R. Heilbronn.** 2003. Adeno-associated virus integrates site-specifically into human chromosome 19 in either orientation and with equal kinetics and frequency. J. Gen. Virol. **84:**133–137.
25. **Jankowski, R. J., and J. Huard.** 2004. Establishing reliable criteria for isolating myogenic cell fractions with stem cell properties and enhanced regenerative capacity. Blood Cells Mol. Dis. **32:**24–33.
26. **Knaän-Shanzer, S., I. van der Velde, M. J. E. Havenga, A. A. C. Lemckert, A. A. F. de Vries, and D. Valerio.** 2001. Highly efficient targeted transduction of undifferentiated human hemopoietic cells by adenoviral vectors displaying fiber knobs of subgroup B. Hum. Gene Ther. **12:**1989–2005.
27. **Kochanek, S., P. R. Clemens, K. Mitani, H. H. Chen, S. Chan, and C. T. Caskey.** 1996. A new adenoviral vector: replacement of all viral coding sequences with 28 kb of DNA independently expressing both full-length dystrophin and β-galactosidase. Proc. Natl. Acad. Sci. USA **93:**5731–5736.
28. **Kochanek, S., G. Schiedner, and C. Volpers.** 2001. High-capacity "gutless" adenoviral vectors. Curr. Opin. Mol. Ther. **3:**454–463.
29. **Kotin, R. M., J. C. Menninger, D. C. Ward, and K. I. Berns.** 1991. Mapping and direct visualization of a region-specific viral DNA integration site on chromosome 19q13-qter. Genomics **10:**831–834.
30. **Kotin, R. M., M. Siniscalco, R. J. Samulski, X. Zhu, L. Hunter, C. A. Laughlin, S. McLaughlin, N. Muzyczka, M. Rocchi, and K. I. Berns.** 1990. Site-specific integration by adeno-associated virus. Proc. Natl. Acad. Sci. USA **87:**2211–2215.
31. **Kumar-Singh, R., and J. S. Chamberlain.** 1996. Encapsidated adenovirus minichromosomes allow delivery and expression of a 14-kb dystrophin cDNA to muscle cells. Hum. Mol. Genet. **5:**913–921.
32. **Linden, R. M., P. Ward, C. Giraud, E. Winocour, and K. I. Berns.** 1996. Site-specific integration by adeno-associated virus. Proc. Natl. Acad. Sci. USA **93:**11288–11294.
33. **McCarty, D. M., D. J. Pereira, I. Zolotukhin, X. Zhou, J. H. Ryan, and N. Muzyczka.** 1994. Identification of linear DNA sequences that specifically bind the adeno-associated virus Rep protein. J. Virol. **68:**4988–4997.
34. **Moisset, P.-A., Y. Gagnon, G. Karpati, and J. P. Tremblay.** 1998. Expression of human dystrophin following the transplantation of genetically modified *mdx* myoblasts. Gene Ther. **5:**1340–1346.
35. **Niwa, H., K.-I. Yamamura, and J.-i. Miyazaki.** 1991. Efficient selection for high-expression transfectants with a novel eukaryotic vector. Gene **108:**193–200.
36. **Parks, R. J., L. Chen, M. Anton, U. Sankar, M. A. Rudnicki, and F. L. Graham.** 1996. A helper-dependent adenovirus vector system: removal of helper virus by Cre-mediated excision of the viral packaging signal. Proc. Natl. Acad. Sci. USA **93:**13565–13570.
37. **Parks, R. J., and F. L. Graham.** 1997. A helper-dependent system for adenovirus vector production helps define a lower limit for efficient DNA packaging. J. Virol. **71:**3293–3298.
38. **Philpott, N. J., C. Giraud-Wali, C. Dupuis, J. Gomos, H. Hamilton, K. I. Berns, and E. Falck-Pedersen.** 2002. Efficient integration of recombinant adeno-associated virus DNA vectors requires a p5-*rep* sequence in *cis*. J. Virol. **76:**5411–5421.
39. **Philpott, N. J., J. Gomos, K. I. Berns, E. Falck-Pedersen.** 2002. A p5 integration efficiency element mediates Rep-dependent integration into AAVS1 at chromosome 19. Proc. Natl. Acad. Sci. USA **99:**12381–12385.
40. **Rademaker, H. J., M. A. Abou El Hassan, G. A. Versteeg, M. J. W. E. Rabelink, and R. C. Hoeben.** 2002. Efficient mobilization of E1-deleted adenovirus type 5 vectors by wild-type adenoviruses of other serotypes. J. Gen. Virol. **83:**1311–1314.
41. **Sambrook, J., and D. W. Russell.** 2001. Molecular cloning: a laboratory manual, 3rd ed. Cold Spring Harbor Laboratory Press, Cold Spring Harbor, N.Y.
42. **Sampaolesi, M., Y. Torrente, A. Innocenzi, R. Tonlorenzi, G. D'Antona, M. A. Pellegrino, R. Barresi, N. Bresolin, M. G. C. De Angelis, K. P. Campbell, R. Bottinelli, and G. Cossu.** 2003. Cell therapy of α-sarcoglycan null dystrophic mice through intra-arterial delivery of mesoangioblasts. Science **301:**487–492.
43. **Samulski, R. J., X. Zhu, X. Xiao, J. D. Brook, D. E. Housman, N. Epstein, and L. A. Hunter.** 1991. Targeted integration of adeno-associated virus (AAV) into human chromosome 19. EMBO J. **10:**3941–3950. (Erratum, 11:1228).
44. **Sandig, V., R. Youil, A. J. Bett, L. L. Franlin, M. Oshima, D. Maione, F. Wang, M. L. Metzker, R. Savino, and C. T. Caskey.** 2000. Optimization of the helper-dependent adenovirus system for production and potency in vivo. Proc. Natl. Acad. Sci. USA **97:**1002–1007.
45. **Scott, J. M., S. Li, S. Q. Harper, R. Welikson, D. Bourque, C. DelloRusso, S. D. Hauschka, and J. S. Chamberlain.** 2002. Viral vectors for gene transfer of micro-, mini-, or full-length dystrophin. Neuromuscul. Disord. **12:**S23–S29.
46. **Seale, P., A. Asakura, and M. A. Rudnicki.** 2001. The potential of muscle stem cells. Dev. Cell **1:**333–342.
47. **Sicinski, P., Y. Geng, A. S. Ryder-Cook, E. A. Barnard, M. G. Darlison, and P. J. Barnard.** 1989. The molecular basis of muscular dystrophy in the *mdx* mouse: a point mutation. Science **244:**1578–1580.
48. **Taboit-Dameron, F., B. Malassagne, C. Viglietta, C. Puissant, M. Leroux-Coyau, C. Chéreau, J. Attal, B. Weill, and L.-M. Houdebine.** 1999. Association of the 5′HS4 sequence of the chicken β-globin locus control region with human EF1α gene promoter induces ubiquitous and high expression of human CD55 and CD59 cDNAs in transgenic rabbits. Transgenic Res. **8:**223–235.
49. **Thomas, C. E., G. Schiedner, S. Kochanek, M. G. Castro, and P. R. Lowenstein.** 2001. Preexisting anti-adenoviral immunity is not a barrier to efficient and stable transduction of the brain, mediated by novel high-capacity adenovirus vectors. Hum. Gene Ther. **12:**839–846.
50. **Tsunoda, H., T. Hayakawa, N. Sakuragawa, and H. Koyama.** 2000. Site-specific integration of adeno-associated virus-based plasmid vectors in lipofected HeLa cells. Virology **268:**391–401.
51. **Umaña, P., C. A. Gerdes, D. Stone, J. R. E. Davis, D. Ward, M. G. Castro, and P. R. Lowenstein.** 2001. Efficient FLPe recombinase enables scalable production of helper-dependent adenoviral vectors with negligible helper-virus contamination. Nat. Biotechnol. **19:**582–585.
52. **van der Wees, C. G. C., M. P. G. Vreeswijk, M. Perssoon, A. van der Laarse, A. A. van Zeeland, and L. H. F. Mullenders.** 2003. Deficient global genome repair of UV-induced cyclobutane pyrimidine dimers in terminally differentiated myocytes and proliferating fibroblasts from the rat heart. DNA Repair **2:**1297–1308.
53. **Ward, P., and K. I. Berns.** 1991. In vitro rescue of an integrated hybrid adeno-associated virus/simian virus 40 genome. J. Mol. Biol. **218:**791–804.
54. **Weitzman, M. D., S. R. M. Kyöstiö, R. M. Kotin, and R. A. Owens.** 1994. Adeno-associated virus (AAV) Rep proteins mediate complex formation between AAV DNA and its integration site in human DNA. Proc. Natl. Acad. Sci. USA **91:**5808–5812.
55. **Xiao, X., W. Xiao, J. Li, and R. J. Samulski.** 1997. A novel 165-base-pair terminal repeat sequence is the sole *cis* requirement for the adeno-associated virus life cycle. J. Virol. **71:**941–948.